DEPARTMENT OF THE INTERIOR

U.S. GEOLOGICAL SURVEY

Sample localities, radiometric ages, descriptions, and major- and trace-element abundances of Late Jurassic mafic plutonic rocks, eastern Sierra Nevada, California

by

Thomas P. Frost

MS 938
345 Middlefield Road
Menlo Park, California 94025

Open-File Report 87-484

1987

Introduction

This report is a compilation of sample localities, radiometric ages, abbreviated sample descriptions, and major- and trace-element determinations of samples from selected mafic plutons from the eastern Sierra Nevada, California, between $36^{o}45'$N and $37^{o}35'$N. Figure 1 is a map of the region under consideration, Figures 2 through 20 are major and trace element Harker plots for the oxides and trace elements vs. silica. Table 1 describes the localities and rock types present at each locality, Table 2 presents sample locality latitude and longitudes for the samples on which major- and trace-element determinations were made. Table 3 presents the major element data. Table 4 presents minor- and trace-element data. Table 5 presents the radiometric age data for mafic rocks of the eastern Sierra Nevada. Fifteen minute USGS quadrangle maps covered are: Casa Diablo Mountain, Mt. Abbot, Mt. Tom, Bishop, Mt. Goddard, Big Pine, Marion Peak, and Mt. Pinchot. Geochemical data for Late Cretaceous mafic intrusions associated with the Lamarck Granodiorite (D and H on Fig. 1) are presented in Frost (1987) and Frost and Mahood (1987).

Geological overview

Numerous calc-alkalic gabbroic through quartz dioritic mafic intrusive complexes are present in the eastern Sierra Nevada of California. The bodies range from discrete intrusive bodies with outcrop areas as large as 25 km^2 to remobilized discontinuous screens and septa between younger felsic plutons. Many of the mafic intrusive complexes may have been more areally extensive prior to disruption caused by emplacement of younger granitoids. The intrusions are compositionally and lithologically heterogeneous and range from distinctively layered olivine-clinopyroxene-hornblende gabbros through hornblende

gabbro to biotite-hornblende diorite and quartz diorite. Anorthosite and peridotite are locally present.

Mafic intrusions believed to be as young as Late Cretaceous are relatively abundant in the eastern Sierra Nevada batholith (Frost and Mahood, 1987, Frost and Mattinson, unpub data); mafic intrusions considered in detail in this report are present exclusively in and among granitoids of Jurassic and Triassic age in the eastern part of the Sierra Nevada batholith (Fig. 1).

Sampling Methods

All coarse grained samples collected in the field weighed at least 5 kg; samples taken from areas accessible by automobile weighed at least 20 kg. Samples were coarsely crushed to thumb-joint size with a steel sledge hammer with the sample sandwiched between at least 5 sheets of blank computer paper. After coarse crushing, the samples were inspected visually and any fragments of computer paper adhering to them was removed. A small tungsten carbide jaw crusher was then used to reduce the samples to 1-3 mm. The interior and exterior of the crusher was scrubbed with a toothbrush and thoroughly blasted with filtered compressed air between each sample. The first several handfuls of each sample passed through the crusher were discarded. After jaw crushing, each sample was repeatedly split in a baffle-splitter to yield a sample of about 70 g.

A tungsten carbide shatterbox was used to pulverize the samples to approximately -200 mesh. Between each sample, the shatterbox was scrubbed with a toothbrush, washed in tap water, and dried with compressed air. Final cleaning was performed by crushing a split of the next sample for one minute. The shatterbox was then emptied, brushed with a clean toothbrush, rinsed in deionized water, and dried before the split to be analysed was loaded for crushing. Crushing times varied between 3 and 5 minutes, with biotite-rich

samples requiring the longer times. Quartz subjected to the same procedure showed measurable contamination in Co and W; contamination by other elements was below detection limits for energy-dispersive x-ray fluorescence (XRF) spectrometry.

X-Ray Fluorescence Spectroscopic Analysis

Major-element determinations were made by standard wavelength-dispersive XRF spectroscopic techniques. Reported abundances were made by averaging two determinations on replicate fused glass discs made with lithium tetraborate flux. A sample-flux ratio of 1:10 was utilized. The complete fusion technique is described in Taggart et al (1987). Determinations were made on a Diano 8600 wavelength-dispersive XRF spectrometer. Calibration curves for the major oxides were made by standard methods described by Taggart et al (1987).

Vanadium abundances reported were made by standard wavelength-dispersive XRF spectroscopic techniques using pressed powder pellets on a Diano 8600 spectrometer. Reported values are averages of at least three determinations per sample. An 85:15 ratio of sample powder to spec-pure methyl cellulose binder was used in the pellets. Sample preparation methods and calibration techniques are described in Fabbi (1970), King et al (1977), and Taggart et al (1987).

Minor- and trace-element abundances reported, other than vanadium, are averages of triplicate determinations on replicate powders made on a Kevex 0700/7000 energy-dispersive x-ray spectrometer; matrix corrections were based on Compton-scatter radiation (Johnson, 1984).

Acknowledgments

Reviewed by B.W. King and D.V. Vivit.

References

Bateman PC (1965) Geology and tungsten mineralization of the Bishop district, California. U.S. Geol. Surv. Prof. Pap. 470, 208 p.

Bateman PC, Moore JG (1965) Geologic map of the Mt. Goddard quadrangle, California U.S. Geological Survey Geologic Quadrangle Map GQ-429.

Chen JH, Moore JG (1979) Late Jurassic Independence dike swarm in eastern California. Geology, v. 7, p. 129-133.

Chen JH, Moore JG (1982) Uranium-lead isotopic ages from the Sierra Nevada batholith, California. Journal of Geophysical Research, v.87B, p. 4761-4784.

Dodge FCW, Moore JG (1968) Occurrence and composition of biotites from the Cartridge Pass pluton of the Sierra Nevada batholith, California. U.S. Geological Survey Professional Paper 600-B, B6-B10.

Evernden JF, Kistler, RW (1970) Chronology of emplacement of Mesozoic batholithic complexes of California and western Nevada. U.S. Geological Survey Professional Paper 623, 42 p.

Fabbi BF (1970) A die for pelletizing samples for x-ray fluorescence analysis. U.S. Geological Survey Prof. Pap. 700-B, B187-B189.

Frost TP (1987) Sample localities, descriptions, major- and trace-element abundances from the Lamarck Granodiorite and associated mafic rocks, Sierra Nevada, California. U. S. Geological Survey Open-File Report 87-193, 38 p.

Frost TP, Mahood GA (1987) Field, chemical, and physical constraints on mafic-felsic magma interaction in the Lamarck Granodiorite, Sierra Nevada, California. Geological Society of America Bulletin, v. 99, p. 272-291.

Johnson RG (1984) Trace element analysis of silicates by means of energy-dispersive X-ray spectrometry. X-ray Spectroscopy, v.13, p. 64-68.

King BS, Espos LF, Fabbi BP (1977) X-ray fluorescence minor- and trace-element analysis of silicate rocks in the presence of large interelement effects. Advances in X-ray Analysis, v. 21, p. 75-88.

Lockwood JP, Lydon, PA (1975) Geologic map of the Mount Abbot quadrangle, central Sierra Nevada, California. U.S. Geological Survey Map GQ-1155.

Moore JG (1963) Geology of the Mt. Pinchot quadrangle, southern Sierra Nevada, California. U.S. Geol. Surv. Bulletin 1130, 152 p.

Moore JN, Foster CT, jr (1980) Lower Paleozoic metasedimentary rocks in the east central Sierra Nevada, California: correlations with Great Basin formations. Geol. Soc. Amer. Bull., v. 91, 37-43.

Rinehart CD, Ross DC (1957) Geology of the Casa Diablo Mountain quadrangle, Mono County, California. U.S. Geological Survey Map GQ-99.

Rinehart CD, Ross DC (1964) Geology and mineral deposits of the Mount Morrison quadrangle, Sierra Nevada, California. U.S. Geological Survey Professional Paper 385, 106 p.

Sawka WN (1985) The geochemistry of differentiation processess in granite magma chambers. unpub Ph.D. dissertation, Australian National University.

Stern TW, Bateman PC, Morgan BA, Newell BA, Peck DL (1981) Isotopic U-Pb ages of zircon from granitoids of the central Sierra Nevada, California. U.S. Geol. Surv. Prof. Pap. 1185, 17 p.

Taggart JE jr, Lindsay JR, Scott BA, Vivit DA, Bartel AJ, Stewart KC (1987) Analysis of geological materials by wavelength dispersive x-ray fluorecense spectroscopy. Chapter 5 in U.S. Geol. Surv. Bulletin 1770, in press.

Tobisch OT, Saleeby JB, Fiske RS (1986) Structural history of continental volcanic arc rocks, eastern Sierra Nevada, California: a case for extensional tectonics. Tectonics, v. 5, p. 65-94.

FIGURE CAPTIONS

Fig. 1. Location and regional geologic map. Sources: Rinehart and Ross, 1957, 1964; Moore, 1963; Bateman, 1965; Bateman and Moore, 1965; Moore and Foster, 1980; Stern et al, 1981; Chen and Moore, 1979, 1982; Frost and Mahood, 1987; Frost and Mattinson, unpub. data; Tobisch et al, 1986)

Fig. 2. Harker diagram, TiO_2, in weight percent. All data recalculated anhydrous. Locality coding: A - Armstrong Canyon; C - Casa Diablo-Rock Creek; K - Keough Hot Springs; M - McMurry Meadows, felsic layers; Z - McMurry Meadows, mafic layers; S - Thibaut-Black Canyon; T - Tungsten Hills; X - Mt. Tom.

Fig. 3. Harker diagram, Al_2O_3. All data as in Fig. 2.

Fig. 4. Harker diagram, FeO* (All iron recalculated as FeO). All data as in Fig. 2.

Fig. 5. Harker diagram, MgO. All data as in Fig. 2.

Fig. 6. Harker diagram, MnO. All data as in Fig. 2.

Fig. 7. Harker diagram, CaO. All data as in Fig. 2.

Fig. 8. Harker diagram, Na_2O. All data as in Fig. 2.

Fig. 9. Harker diagram, K_2O. All data as in Fig. 2.

Fig. 10. Harker diagram, P_2O_5. All data as in Fig. 2.

Fig. 11. Harker diagram, Ba (in ppm). All other data as in Fig. 2.

Fig. 12. Harker diagram, Cr (in ppm). Samples shown as zero did not have Cr determined. All other data as in Fig. 2.

Fig. 13. Harker diagram, Nb (in ppm). All other data as in Fig. 2.

Fig. 14. Harker diagram, Ni (in ppm). All other data as in Fig. 2.

Fig. 15. Harker diagram, Rb (in ppm). All other data as in Fig. 2.

Fig. 16. Harker diagram, Sr (in ppm). All other data as in Fig. 2.

Fig. 17. Harker diagram, V (in ppm). All other data as in Fig. 2.

Fig. 18. Harker diagram, Y (in ppm). All other data as in Fig. 2.

Fig. 19. Harker diagram, Zn (in ppm). All other data as in Fig. 2.

Fig. 20. Harker diagram, Zr (in ppm). All other data as in Fig. 2.

Table 1. Age constraints and lithology summary, eastern Sierra Nevada mafic intrusions.

Key to Fig. 1 and Locality	Age	Constraint	Lithologies present	References
1. Casa Diablo-Rock Creek	210-148 (?)my	1, 4	ol gabbro, two-px-ol. gabbro, cpx-hb gabbro, bio-hb diorite bio-hb qtz diorite	3,4,11,16
2. Wheeler Crest	210-148 my	1,4	cpx-hb gabbro, hb gabbro, bio-hb gabbro	1,3,4,16
3. Pine Creek	169 m.y.	U-Pb zircon	bio-hb qtz diorite	1,14
4. Mt. Tom	>148 my	1,4	hb gabbro, hb diorite, bio-hb qtz diorite	1,3,4,16
5. Tungsten Hills	150 my	U-Pb zircon	cpx(hb) gabbro, hb gabbro, hb diorite	1,4,14,16
6. Bishop Creek-Habeggar's	210-148 my	1,4	cpx-hb gabbro, hb gabbro, bio-hb gabbro	1,3,4,16
7. Keough Hot Springs	>148 my	1	ol-cpx (hb) gabbro, hb gabbro	1,14,16
8. Shannon Canyon	167-148 my	1,4	cpx (hb) gabbro, hb gabbro, bio-hb diorite, qtz diorite	1,3,4,16
9. McMurray Meadows	150 my	U-Pb zircon	ol-cpx (hb) gabbro, hb gabbro, bio-hb diorite	1,14,16
10. Armstrong Canyon	154 my	U-Pb zircon	cpx-hb gabbro, hb gabbro, bio-hb gabbro, qtz diorite	3,4,10,16
11. Thibaut-Black Canyon	165-148 my	1, 4	cpx-hb gabbro, hb gabbro, bio-hb gabbro, qtz diorite, anorthosite	3,4,10,16
12. Baxter Lakes	165(?)-148 my	1, 4	cpx-hb gabbro, hb gabbro, hb diorite	3,4,10,16
13. Wood Creek	>148 my	1	hb gabbro, hb diorite	3,4,10,16
Other Mafic Intrusions				
A. Mt. Morrison Pendant	Post-Late Pz	6	Hb diorite	12
B. Hidden Lakes	Late Cretaceous(?)	2(?), 3, 4	Hb gabbro,bio-hb diorite	1,8,9,12,14
C. Pine Lake	97.5 m.y.	U-Pb zircon	Hb diorite - qtz diorite	8,15
D. Piute Pass-Lake Sabrina	Late Cretaceous	4, 5	hb gabbro - mafic grd	1,7,14
E. Black Giant	147-81 m.y. (?)	3, 6	hb gabbro	2,4,6,13,14
F. Green Lake	Late Cretaceous(?)	2(?), 5	hb gabbro - mafic grd	1,7,15
G. Mt. Alice	Late Cretaceous(?)	2(?), 4	hb diorite - qtz diorite	1,15
H. Palisade Creek-Upper Basin	Late Cretaceous	4, 5	hb gabbro - mafic grd	1,5,6,7,14
J. Onion Valley-Rae Lakes	Early Cretaceous(?)	4, 5	Hb diorite - qtz diorite	10,13

Constraint code: 1) older than Independence dikes, 2) younger than Independence dikes, 3) older than surrounding dated granitoids, 4) younger than surrounding granitoids, 5) mutually cross-cutting relations and hybridization with surrounding plutons suggestive of similar age (Frost and Mahood, 1987), 6) intrusive into metamorphic rocks.

References: 1, Bateman, 1965; 2) Bateman and Moore, 1965; 3) Chen and Moore, 1979; 4) Chen and Moore, 1982; 5) Dodge and Moore, 1968; 6) Evernden and Kistler, 1970; 7) Frost and Mahood, 1987; 8) Frost and Mattinson, 19XX; 9) Lockwood and Lydon, 1975: 10) Moore, 1963; 11) Rinehart and Ross, 1957; 12) Rinenart and Ross, 1964; 13) Tobisch and others 1986; 14) Stern and others, 1981; 15) Frost, unpub. data; 16) this report.

Table 2. Sample localities and descriptions, mafic rocks of the eastern Sierra Nevada.

Sample	N. Lat	W. Long	Description
TUNGSTEN HILLS			
TH-D	37.21'25"	118.32'00"	Coarse, massive, poikilitic hornblende gabbro.
TH2-10	37.21'20	118.31'50"	Fine, massive, hypidiomorphic hornblende diorite.
TH2-16	37.21'40"	118.31'40"	Fine, massive, hypidiomorphic hb diorite.
TH2-17	37.21'40"	118.31'40"	Vertically-layered, poikilitic hb gabbro.
TH2-20	37.21'10"	118.32'00"	Porphyritic hb gabbro.
TH2-22	37.21'15"	118.31'40"	Hypidiomorphic hb diorite of Tungsten Blue Mine.
TH2-23	37.20'55"	118.32'00"	Poikilitic, massive hb gabbro.
TH2-27	37.20'00"	118.32'00"	Hypidiomorphic, massive hornblende diorite.
TH2-29	37.21'00"	118.32'00"	Hypidiomorphic, coarse hornblende diorite.
TH2-33	37.21'00"	118.32'00"	Leucocratic, hypidiomorphic hornblende diorite.
TH2-36	37.21'00	118.32'00"	Fine grained, leucocratic microgabbro.
CASA DIABLO			
CD79-1c	37.35'00"	118.40'00"	Layered, biotite-rich, hornblende gabbro.
CD-2	37.35'00"	118.40"00"	Cumulus ol-cpx-hb gabbro. Ol altered to iddingsite.
CD-4	37.35'00"	118.40"00"	Layered cumulus ol-cpx-hb gabbro.
CD-9	37.35'00"	118.40"00"	Coarse ol-cpx-hb gabbro. Kelyphitic hb-pl rims on ol.
CD-11	37.35'00"	118.40"00"	Medium-grained hypidiomorphic hornblende gabbro.
CD-13	37.35'00"	118.40"00"	Fine-grained bio-hb quartz diorite.
CD-15	37.35'00"	118.40"00"	Coarse hornblende gabbro.
CD-17	37.35'00"	118.40"00"	Coarse hornblende gabbro. Hb is euhdral, randomly oriented, cored by aggregate of pl+hb.
CD-21	37.35'00"	118.40"00"	Coarse ol-cpx-hb gabbro. Ol is rimmed by radial growths of pl+cpx+pl.
KEOUGH HOT SPRINGS			
KHS-10A	37.15'05"	118.23'40"	Massive biotite-hornblende diorite.
KHS-11A	37.15'05"	118.23'42"	Coarse lens of hornblende gabbro in finer hb diorite.
KHS-12	37.15'10"	118.23'45"	Faintly layered hypidiomorphic hornblende gabbro.
KHS-17	37.15'40"	118.23'03"	Homogeneous hornblende gabbro.
KHS-19	37.15'30"	118.23'30"	Coarse, homogeneous hornblende gabbro.
KHS-19B	37.15'30"	118.23'30"	Mafic hornblende gabbro in gradational contact with KHS 1-19.
KHS-24	37.15'25"	118.23'30"	Coarse, felsic homogeneous hornblende gabbro.
KHS-33	37.15'10"	118.22'40"	Layered hornblende gabbro.
THIBAUT-BLACK CANYON			
SM-1C	36.52"10"	118.20'30"	Layered, hypidiomorphic biotite-hornblende granodiorite.
SM-3	36.51'05"	118.20'25"	Hornblende-plagioclase pegmatite.
SM-7A	36.52'00"	118.20'10"	Homogeneous, felsic biotite-hornblende diorite
SM-7B	36.52'00"	118.20'10"	Anorthosite (7% hornblende+epidote, remainder is euhedral plagioclase in random orientation, up to 4 mm).
SM-7C	36.52'00"	118.20'10"	Anorthosite similar to SM-7B.
SM-8	36.52'00"	118.20'10"	Anorthosite, color index 3 (hb+epidote). Euhedral pl to 5 mm in random orientation.

Table 2. Continued.

SM-9	36.52'00"	118.20'10"	Anorthosite, color index 3 (hb+epidote). Euhedral pl to 5 mm in random orientation.
SM-10	36.52'05"	118.20'15"	Biotite-hornblende gabbro, sharply cut by dikes of SM-9 type rock.
SM-16	36.52'20"	118.17'30"	Biotite-hornblende mafic granodiorite.
SM-19	36.52'20"	118.17'35"	Biotite-hornblende quartz diorite.
ARMSTRONG CANYON			
AC-8A	36.56'10"	118.20'30"	Coarse hornblende gabbro.
AC-9	36.56'15"	118.20'30"	Coarse hornblende diorite.
AC-21A	36.57'35"	118.20'30"	Coarse, mafic, hornblende gabbro at contact with younger Goodale pluton of Moore (1963).
AC-21C	36.57'35"	118.20'30"	Coarse, "spotted" (poikilitic) hornblende gabbro.
AC-21D	36.57'35"	118.20'30"	Crudely-layered biotite-hornblende gabbro.
AC-23	36.57'25"	118.20'50"	Faintly-layered biotite-hornblende, medium grained diorite.
AC-26B	36.57'20"	118.21'20"	Coarse, biotite-hornblende quartz diorite. Dating sample from Armstrong Canyon is similar to this sample.
AC-27	36.57'15"	118.21'20"	Fine-grained homogeneous hornblende gabbro.
AC-29	36.57'00"	118.22'00"	Homogeneous, hypidiomorphic biotite-hornblende diorite.
MT. TOM			
T-3	37.20'30"	118.38'30"	Massive, medium-grained, hornblende diorite.
T-5	37.20'30"	118.38'30"	Massive, medium-grained, hornblende gabbro.
T-7	37.20'30"	118.38'30"	Massive, medium-grained, hornblende diorite.
T-10	37.20'30"	118.38'30"	Massive, medium-grained, hornblende diorite.
McMURRY MEADOWS			
McM-D	37.04'00"	118.21'05"	Homogeneous, medium grained hornblende gabbro.
McM-1D	37.04'40"	118.21'05"	Coarse, cumulus hb gabbro. Original cpx altered to hornblende.
McM-1E	37.04'40"	118.21'05"	Poikilitic, mafic, hornblende gabbro.
McM-7A	37.04'00"	118.22'10"	Poikilitic, mafic, horizontal-layered, coarse hornblende gabbro.
McM-8	37.04'05"	118.22'30"	Poikilitic, mafic, horizontal-layered, coarse hornblende gabbro.
McM-11	37.04'10"	118.23'00"	Felsic, faintly horizontal-layered, coarse, poikilitic hornblende gabbro.
McM-15C	37.04'10"	118.23'10"	Plagioclase-rich layer in horizontal-layered hb gabbro.
McM-16	37.04'05"	118.23'00"	Mafic layer in horizontal-layered poikilitic hornblende gabbro.
McM-18	37.04'05"	118.22'55"	Homogeneous, poikilitic hornblende gabbro.
McM-19	37.04'05"	118.22'55"	Homogeneous, poikilitic hornblende gabbro.
McM-23	37.04'35"	118.22'00"	Coarse, felsic hornblende gabbro.
McM-25	37.04'00"	118.21'05"	Coarse, porphyritic hornblende gabbro. Faint horizontal layering visible locally.
McM-32	37.04'00"	118.21'05"	Well-layered hornblende gabbro. Mafic facies.
PAL11	37.04'30"	118.22'40"	Felsic layer in hornblende gabbro.
PAL12	37.04'30"	118.22'40"	Mafic hornblende gabbro.
PAL13	37.04'30"	118.22'40"	Mafic hornblende gabbro.

Table 3. Major element determinations.

	SiO2	TiO2	Al2O3	Fe2O3	MnO	MgO	CaO	Na2O	K2O	P2O5	LOI	TOTAL
TH-D	48.10	0.28	24.50	4.91	0.08	4.87	14.20	1.41	0.61	0.05	1.16	100.17
TH-2-10	50.20	0.65	17.30	9.44	0.17	7.50	9.02	2.33	0.82	0.12	2.41	99.96
TH-2-16	52.80	0.82	19.00	9.28	0.16	4.43	8.30	2.96	0.97	0.29	0.85	99.87
TH-2-17	42.40	1.02	20.40	13.30	0.11	5.99	14.20	0.99	0.22	0.05	1.28	99.96
TH-2-20	53.00	0.50	7.66	9.88	0.20	12.70	12.80	0.74	0.30	0.14	1.08	99.00
TH-2-22	53.50	0.76	20.10	7.92	0.13	3.88	8.93	3.09	1.17	0.25	0.38	100.11
TH-2-23	45.90	0.54	26.70	6.69	0.07	3.48	14.40	1.78	0.14	0.05	0.37	100.12
TH-2-27	56.50	0.72	18.00	7.74	0.15	3.79	7.10	3.39	1.45	0.24	0.64	99.72
TH-2-29	52.40	0.92	18.80	9.67	0.17	4.15	8.71	2.50	1.29	0.38	0.80	99.79
TH-2-33	55.50	0.90	19.80	3.18	0.09	2.37	9.78	3.36	3.08	0.35	0.80	99.21
TH-2-36	57.60	0.72	17.50	7.18	0.14	3.27	6.71	3.06	2.38	0.22	0.59	99.31
CD-79-1C	47.20	0.82	24.50	8.10	0.09	2.79	11.20	2.52	0.69	0.20	1.68	99.79
CD-2	40.90	0.34	9.99	16.80	0.24	22.30	8.40	0.42	0.08	0.05	0.58	100.10
CD-4	40.80	0.72	18.20	13.40	0.13	11.10	13.00	0.62	0.15	0.05	1.90	100.07
CD-9	40.70	0.10	17.90	12.40	0.16	17.00	9.61	0.51	0.06	0.05	1.81	99.70
CD-11	44.00	1.44	19.00	12.10	0.12	7.46	10.90	1.97	0.93	0.12	1.78	99.82
CD-13	51.60	0.97	19.20	9.18	0.16	4.75	9.35	3.18	0.90	0.34	0.31	99.94
CD-15	40.00	2.40	12.20	18.80	0.20	12.10	10.70	1.55	0.61	0.06	0.89	99.51
CD-17	45.00	1.72	15.80	13.30	0.13	9.02	10.20	2.19	1.06	0.11	0.83	99.36
CD-21	41.40	0.63	20.90	11.00	0.13	10.10	12.70	0.86	0.24	0.05	2.00	100.01
KHS-1-10A	54.50	0.94	18.90	8.32	0.13	3.73	7.68	3.46	1.84	0.33	0.36	100.19
KHS-1-11A	49.20	1.08	18.30	11.10	0.17	6.01	9.87	2.82	0.50	0.36	0.63	100.04
KHS-1-12A	53.40	0.98	18.40	8.98	0.14	4.65	8.10	3.31	1.36	0.30	0.44	100.06
KHS-1-17	45.00	1.27	20.50	11.10	0.12	6.10	11.20	2.16	1.05	0.13	1.41	100.04
KHS-1-19	48.80	1.11	13.80	11.50	0.16	10.10	11.10	1.81	0.93	0.08	0.81	100.20
KHS-1-19B	47.60	1.00	16.70	11.40	0.17	8.35	11.00	2.06	0.65	0.20	0.39	99.52
KHS-1-24	54.50	0.80	20.30	6.71	0.09	2.96	7.67	3.58	1.87	0.41	0.80	99.69
KHS-1-33	46.60	0.95	16.80	7.97	0.10	9.04	16.00	1.32	0.48	0.05	0.86	100.17
SM-1C	60.30	0.51	20.40	3.33	0.04	1.50	5.94	4.74	2.38	0.17	0.39	99.70
SM-3	39.90	2.33	14.40	19.70	0.17	7.90	13.70	1.15	0.30	0.06	0.57	100.18
SM-7A	49.40	1.22	20.60	9.14	0.13	4.78	9.88	3.08	0.38	0.29	1.50	100.40
SM-7B	49.80	0.94	25.70	5.68	0.05	1.44	11.50	3.56	0.50	0.14	1.11	100.42
SM-7C	50.30	0.50	27.60	3.26	0.03	1.25	12.40	3.60	0.32	0.05	0.91	100.22
SM-8	46.10	0.39	30.10	3.58	0.02	0.97	15.50	1.69	0.46	0.08	1.15	100.04
SM-9	48.80	0.46	28.70	3.62	0.02	1.17	13.70	2.83	0.28	0.05	0.93	100.56
SM-10	43.10	2.11	19.10	12.70	0.12	7.16	11.20	2.04	0.95	0.16	1.28	99.92
SM-16	61.60	0.67	16.30	5.79	0.10	2.45	4.93	3.40	3.69	0.30	0.36	99.59
SM-19	57.30	1.09	16.90	7.64	0.12	3.38	6.10	3.57	3.16	0.34	0.22	99.82
AC-8A	44.10	1.78	17.40	14.50	0.17	6.30	10.90	2.05	0.87	0.15	2.07	100.29
AC-9	53.60	0.85	18.60	8.59	0.16	4.24	8.38	3.02	1.46	0.25	0.82	99.97
AC-21A	47.40	1.01	21.70	10.10	0.14	3.44	9.05	3.59	1.60	0.71	1.06	99.80
AC-21C	49.90	1.42	16.90	11.20	0.14	5.65	7.43	2.63	2.26	0.31	1.34	99.18
AC-21D	46.20	1.53	18.30	13.10	0.19	5.73	8.65	2.59	2.15	0.52	1.06	100.02
AC-23	47.60	1.20	19.60	11.20	0.16	5.24	9.14	3.16	1.56	0.45	0.73	100.04
AC-26B	62.30	0.70	16.70	5.30	0.04	2.94	3.94	3.92	2.63	0.33	0.69	99.49
AC-27	47.90	1.49	18.70	11.70	0.13	5.06	8.06	3.04	2.00	0.31	1.30	99.69
AC-29	52.30	1.03	16.40	8.73	0.14	6.45	8.85	2.49	2.00	0.21	1.39	99.99
T-3	53.80	0.89	17.30	9.16	0.16	4.91	8.42	2.73	1.36	0.24	0.54	99.51
T-5	50.00	0.68	15.00	11.00	0.21	9.27	10.70	1.65	0.72	0.10	0.58	99.91
T-7	51.60	0.58	17.10	9.15	0.17	7.70	9.84	1.90	0.85	0.11	1.00	100.00
T-10	52.10	0.70	16.60	9.76	0.18	7.26	9.38	2.00	1.04	0.14	0.70	99.86
MCM-D	48.20	0.49	17.30	7.61	0.13	8.14	15.50	1.07	0.39	0.08	1.10	100.01
MCM-1D	49.70	0.61	10.60	9.17	0.16	11.50	15.50	0.97	0.57	0.11	0.96	99.85
MCM-1E	46.60	0.94	10.50	12.90	0.15	10.90	16.00	0.83	0.40	0.05	0.70	99.97
MCM-7A	48.60	0.69	11.30	9.01	0.15	11.20	16.30	1.18	0.46	0.09	0.78	99.75
MCM-8	50.80	0.67	9.36	8.24	0.16	11.30	16.70	1.15	0.56	0.12	0.99	100.05
MCM-11	45.00	0.36	20.90	7.94	0.11	8.36	14.30	0.97	0.31	0.05	1.86	100.16
MCM-15C	47.90	0.69	12.80	8.81	0.14	10.60	16.50	1.10	0.34	0.07	0.83	99.78
MCM-16	49.40	0.57	8.41	9.20	0.16	13.60	16.20	0.82	0.36	0.08	0.86	99.66
MCM-18	49.50	0.62	17.70	7.28	0.13	7.70	13.70	1.51	0.50	0.17	1.29	100.10
MCM-19	48.80	0.54	18.60	6.66	0.12	6.81	14.70	1.36	0.62	0.13	1.29	99.63
MCM-23	48.70	0.63	16.50	7.36	0.13	8.63	14.30	1.46	0.73	0.12	1.19	99.75
MCM-25	49.80	0.70	6.99	10.10	0.18	14.10	15.40	0.97	0.42	0.12	0.79	99.57
MCM-32	48.40	0.58	10.20	8.86	0.16	13.20	16.20	0.74	0.27	0.07	1.16	99.84
PAL11	48.23	0.50	15.63	6.13	0.10	8.40	17.20	1.41	0.23	0.06		97.89
PAL12	49.91	0.71	8.70	8.82	0.15	12.09	15.90	1.19	0.44	0.09	1.63	99.63
PAL13	46.48	0.91	9.87	11.21	0.17	11.94	16.90	0.95	0.18	0.04	1.40	100.05

Table 4. Trace element determinations. Reported values in ppm.

	V	CR	NI	ZN	RB	SR	Y	ZR	NB	BA
TH-D	100	110	20	46	31	635	13	41	3	240
TH-2-10	230	0	50	90	33	500	15	54	2	540
TH-2-16	195	28	16	110	23	620	17	65	6	625
TH-2-17	410	0	17	69	14	620	10	34	2	170
TH-2-20	250	0	160	125	11	270	13	48	2	280
TH-2-22	175	29	19	81	23	575	22	81	5	630
TH-2-23	260	0	29	43	14	780	7	32	2	140
TH-2-27	170	0	23	97	38	520	20	145	2	1000
TH-2-29	230	28	13	110	41	600	23	88	7	720
TH-2-33	0	0	13	83	93	825	20	60	2	5000
TH-2-36	160	0	23	100	58	450	24	140	2	1500
CD-79-1C	200	0	10	60	34	855	16	59	2	480
CD-2	140	365	165	115	11	305	6	19	2	85
CD-4	325	140	66	89	11	590	6	29	2	120
CD-9	60	360	125	99	11	620	4	25	2	77
CD-11	400	72	25	92	31	700	16	58	4	445
CD-13	210	40	21	114	29	821	15	95	5	800
CD-15	625	260	52	135	17	260	23	59	2	250
CD-17	450	110	35	90	25	525	18	65	7	490
CD-21	225	115	66	93	12	790	7	30	3	125
KHS-1-10A	175	10	20	110	55	740	19	125	8	1080
KHS-1-11A	260	45	26	140	18	850	15	59	5	505
KHS-1-12A	210	46	25	100	44	720	17	110	8	810
KHS-1-17	370	0	18	105	34	670	19	66	2	355
KHS-1-19	265	0	89	115	34	450	14	61	2	1040
KHS-1-19B	320	110	57	120	36	750	11	50	5	395
KHS-1-24	150	0	10	95	72	780	17	125	2	1030
KHS-1-33	250	0	86	61	13	600	13	54	2	220
SM-1C	73	0	10	43	71	750	16	170	2	820
SM-3	610	0	12	110	14	570	12	49	2	215
SM-7A	245	44	25	110	15	1020	9	40	4	495
SM-7B	150	5	11	45	20	1250	11	60	4	600
SM-7C	97	5	13	30	17	1270	12	44	3	525
SM-8	80	5	8	22	21	1370	12	61	3	275
SM-9	95	5	9	21	15	1100	11	51	4	370
SM-10	470	90	57	69	30	800	16	69	6	365
SM-16	115	10	16	55	100	635	22	134	12	1150
SM-19	160	44	36	84	125	540	25	180	12	780
AC-8A	550	45	17	82	45	450	19	84	5	270
AC-9	210	38	21	86	40	475	22	110	7	670
AC-21A	135	0	13	145	64	1000	23	205	2	1130
AC-21C	290	0	38	120	70	880	23	175	2	1210
AC-21D	290	0	29	155	60	860	25	175	2	1250
AC-23	220	39	25	130	49	830	25	185	11	530
AC-26B	125	11	14	35	122	622	22	150	11	1000
AC-27	285	0	45	148	60	720	21	170	2	1120
AC-29	270	0	40	105	64	540	21	110	2	750
T-3	240	70	21	94	42	500	19	74	8	750
T-5	252	150	42	100	29	430	14	45	5	350
T-7	210	120	34	84	31	495	12	63	5	480
T-10	245	105	34	100	38	480	17	69	4	560
MCM-D	185	65	77	62	12	700	12	50	4	165
MCM-1D	235	740	140	64	17	300	14	45	6	210
MCM-1E	485	500	78	63	12	320	12	42	3	160
MCM-7A		460	110	60	14	350	14	53	5	150
MCM-8	265	900	133	44	16	280	14	64	3	170
MCM-11	150	40	86	53	16	650	8	39	3	110
MCM-15C	265	370	74	46	12	360	12	43	4	165
MCM-16	245	310	190	59	12	230	13	44	3	165
MCM-18	215	180	61	62	13	535	12	54	5	275
MCM-19	195	60	69	58	20	575	14	56	3	270
MCM-23	200	180	84	60	27	500	14	60	4	230
MCM-25	265	370	185	65	11	200	15	48	3	225
MCM-32	220	250	155	57	9	260	10	43	3	120
PAL11	0	173	123	38	5	494	10	35	1	0
PAL12	0	274	140	59	10	225	16	48	3	0
PAL13	0	277	118	70	4	295	14	33	1	96

Table 5. U-Pb zircon ages, eastern Sierra Nevada mafic plutonic rocks.

Intrusion Number and Sample		U^{238} (ppm)	Pb^{206*} (ppm)	$\frac{Pb^{208}}{Pb^{206}}$[1]	$\frac{Pb^{207}}{Pb^{206}}$[1]	$\frac{Pb^{204}}{Pb^{206}}$[1]	$\frac{Pb^{206*}}{U^{238}}$[2]	$\frac{Pb^{207*}}{U^{235}}$[2]	$\frac{Pb^{207*}}{Pb^{206*}}$[2]
Mafic intrusions									
5	TH-D	384.3	7.846	0.2363	0.05150	0.0001596	150.3	150.6	155±8
9	McM-D	1397.1	28.64	0.3968	0.05035	0.0000842	150.8	151.0	154±7
10	AC	573.9	12.00	0.2044	0.05297	0.000246	153.8	154.5	165±10
Tungsten Hills Granite									
	THG	1658.0	41.12	0.1031	0.05068	0.0000477	182.0	182.8	194±4

* Radiogenic lead. [1] Isotopic ratios corrected for fractionation. [2] Age in 10^6 years. Uncertainty in 206*/238 and 207*/235 ages are 1 per cent.

FIGURE CAPTIONS

Fig. 1. Location and regional geologic map. Sources: Rinehart and Ross, 1957, 1964; Moore, 1963; Bateman, 1965; Bateman and Moore, 1965; Moore and Foster, 1980; Stern et al, 1981; Chen and Moore, 1979, 1982; Frost and Mahood, 1987; Frost and Mattinson, in prep; Tobisch et al, 1986)

Fig. 2. Harker diagram, TiO_2, in weight percent. All data recalculated anhydrous. Locality coding: A - Armstrong Canyon; C - Casa Diablo-Rock Creek; K - Keough Hot Springs; M - McMurry Meadows, felsic layers; Z - McMurry Meadows, mafic layers; S - Thibaut-Black Canyon; T - Tungsten Hills; X - Mt. Tom.

Fig. 3. Harker diagram, Al_2O_3. All data as in Fig. 2.

Fig. 4. Harker diagram, FeO* (All iron recalculated as FeO). All data as in Fig. 2.

Fig. 5. Harker diagram, MgO. All data as in Fig. 2.

Fig. 6. Harker diagram, MnO. All data as in Fig. 2.

Fig. 7. Harker diagram, CaO. All data as in Fig. 2.

Fig. 8. Harker diagram, Na_2O. All data as in Fig. 2.

Fig. 9. Harker diagram, K_2O. All data as in Fig. 2.

Fig. 10. Harker diagram, P_2O_5. All data as in Fig. 2.

Fig. 11. Harker diagram, Ba (in ppm). All other data as in Fig. 2.

Fig. 12. Harker diagram, Cr (in ppm). Samples shown as zero did not have Cr determined. All other data as in Fig. 2.

Fig. 13. Harker diagram, Nb (in ppm). All other data as in Fig. 2.

Fig. 14. Harker diagram, Ni (in ppm). All other data as in Fig. 2.

Fig. 15. Harker diagram, Rb (in ppm). All other data as in Fig. 2.

Fig. 16. Harker diagram, Sr (in ppm). All other data as in Fig. 2.

Fig. 17. Harker diagram, V (in ppm). All other data as in Fig. 2.

Fig. 18. Harker diagram, Y (in ppm). All other data as in Fig. 2.

Fig. 19. Harker diagram, Zn (in ppm). All other data as in Fig. 2.

Fig. 20. Harker diagram, Zr (in ppm). All other data as in Fig. 2.

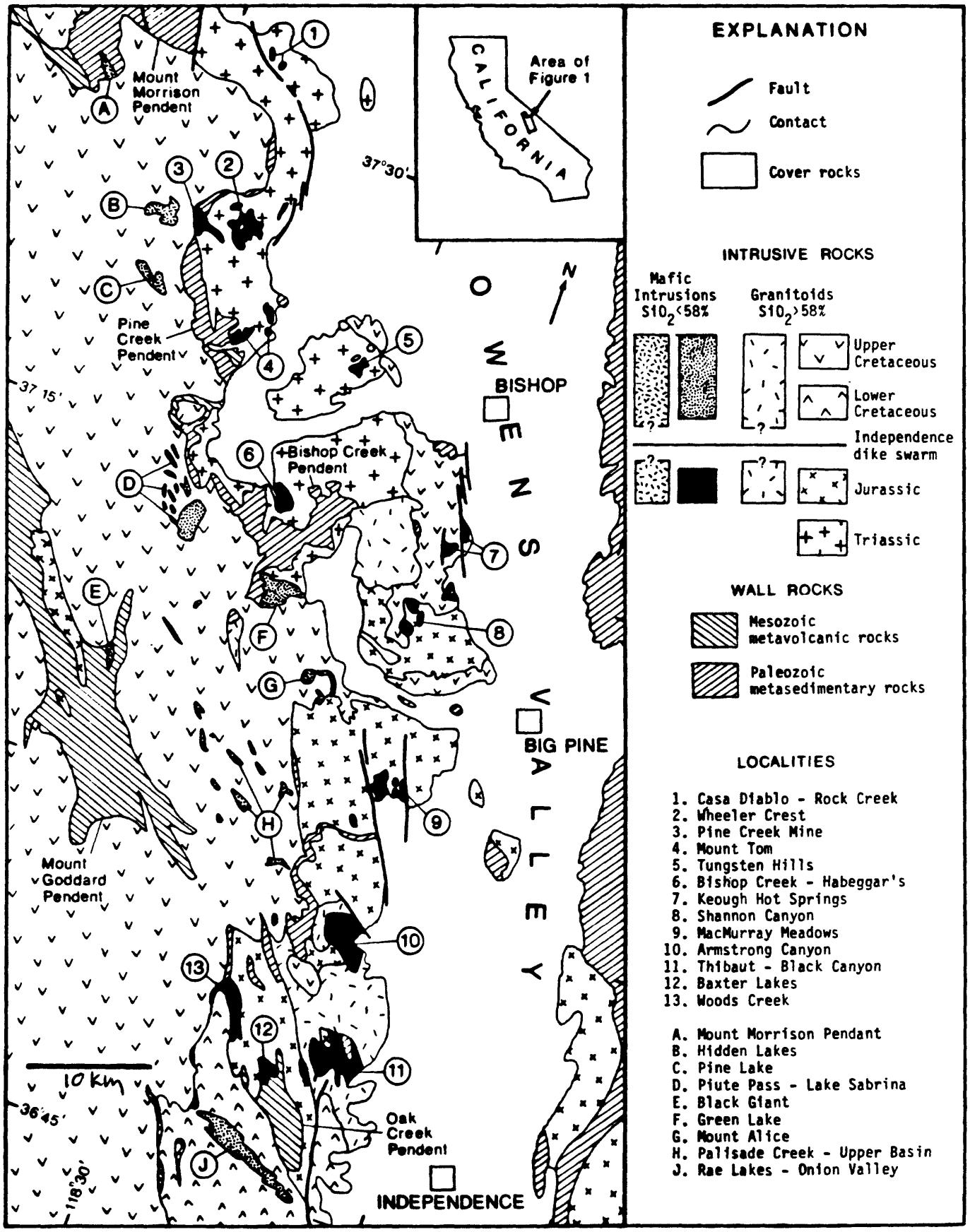
Mount Morrison Pendent
Pine Creek Pendent
Bishop Creek Pendent
Mount Goddard Pendent
Oak Creek Pendent
BISHOP
BIG PINE
INDEPENDENCE
OWENS VALLEY
Area of Figure 1
CALIFORNIA
37°30'
37°15'
36°45'
118°30'
10 km
N
EXPLANATION
Fault
Contact
Cover rocks
INTRUSIVE ROCKS
Mafic Intrusions SiO2<58%
Granitoids SiO2>58%
Upper Cretaceous
Lower Cretaceous
Independence dike swarm
Jurassic
Triassic
WALL ROCKS
Mesozoic metavolcanic rocks
Paleozoic metasedimentary rocks
LOCALITIES
1. Casa Diablo - Rock Creek
2. Wheeler Crest
3. Pine Creek Mine
4. Mount Tom
5. Tungsten Hills
6. Bishop Creek - Habeggar's
7. Keough Hot Springs
8. Shannon Canyon
9. MacMurray Meadows
10. Armstrong Canyon
11. Thibaut - Black Canyon
12. Baxter Lakes
13. Woods Creek
A. Mount Morrison Pendant
B. Hidden Lakes
C. Pine Lake
D. Piute Pass - Lake Sabrina
E. Black Giant
F. Green Lake
G. Mount Alice
H. Palisade Creek - Upper Basin
J. Rae Lakes - Onion Valley

Fig. 1

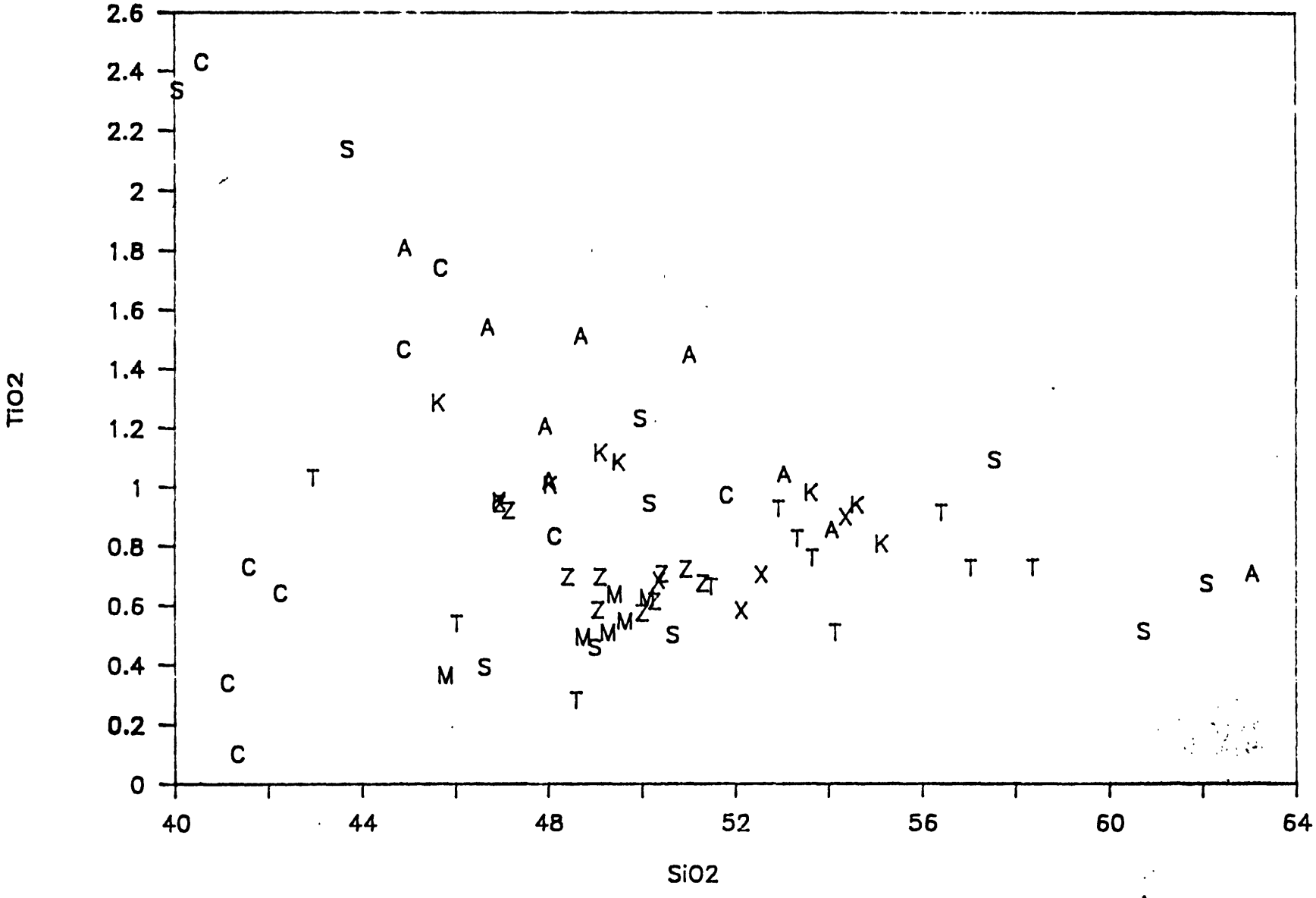

Fig. 2

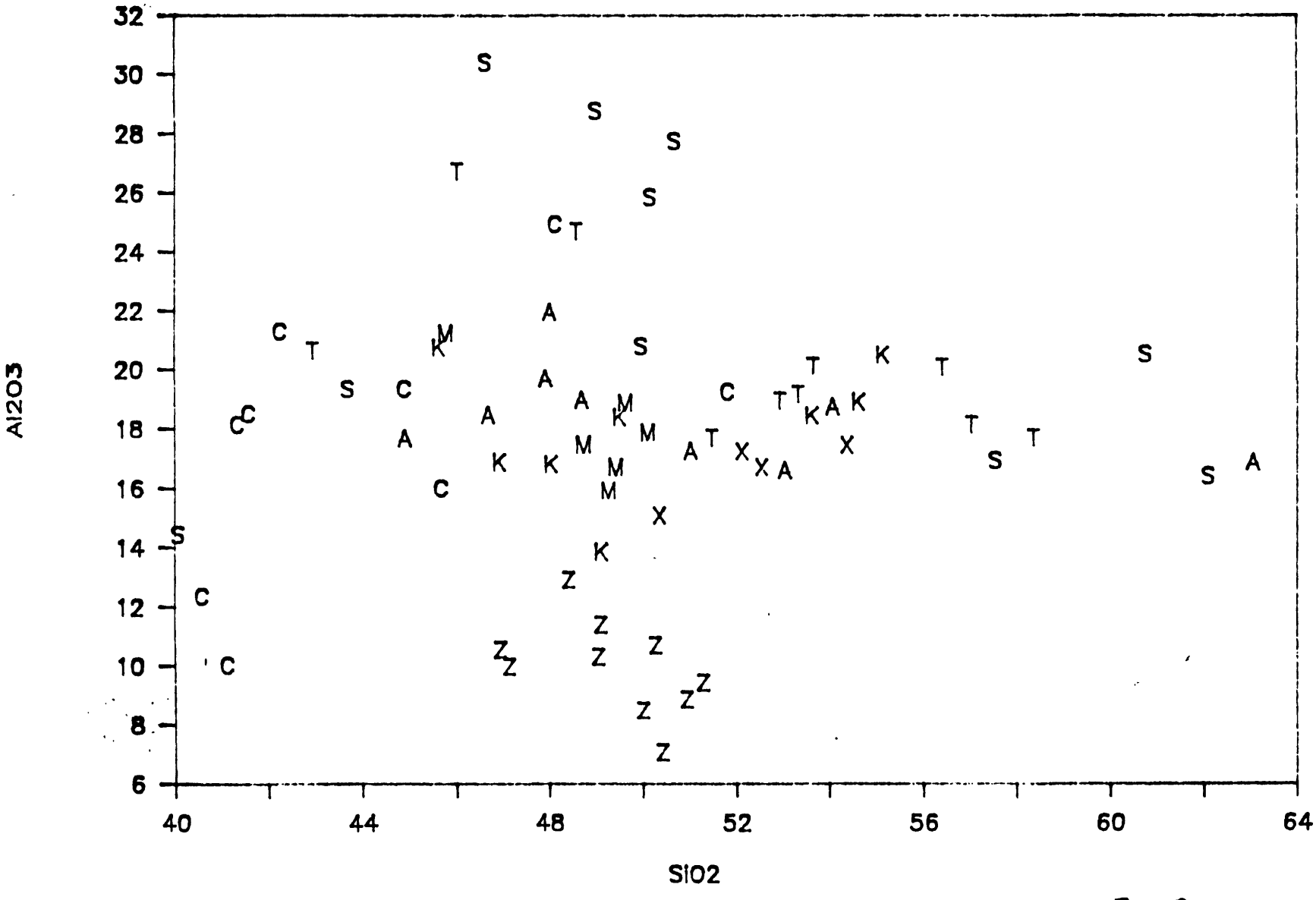

Fig. 3

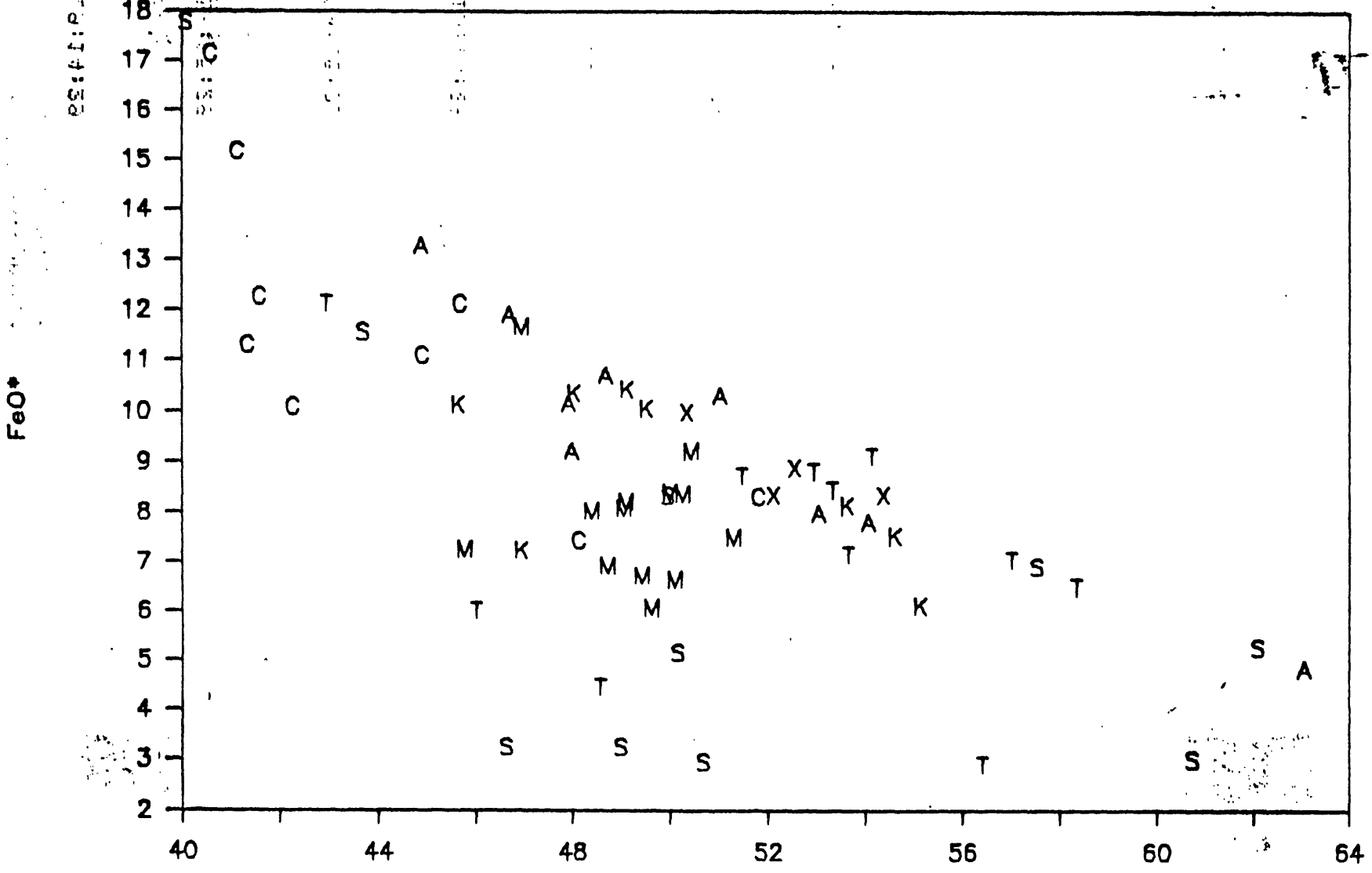

Fig. 4

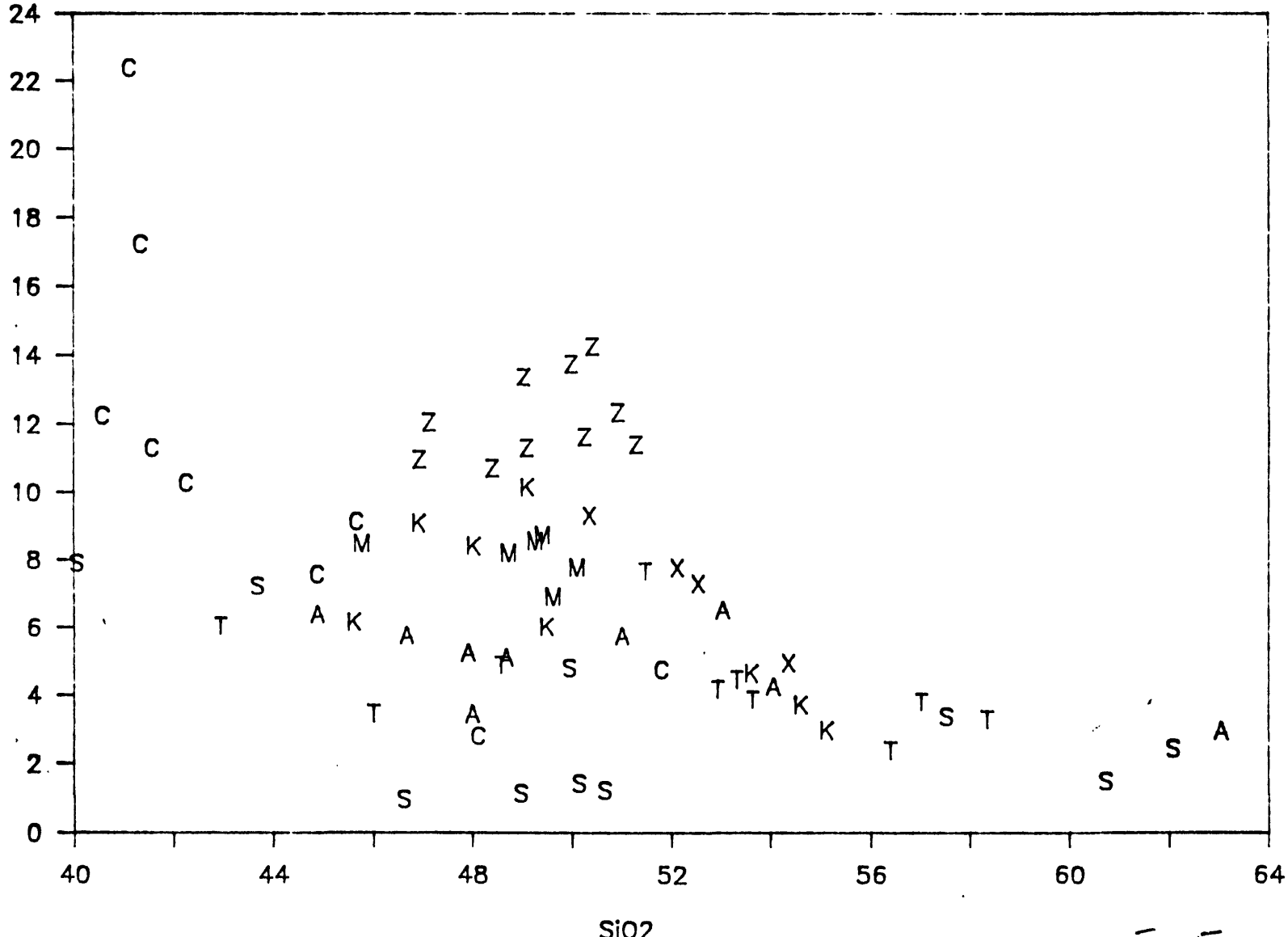

Fig. 5

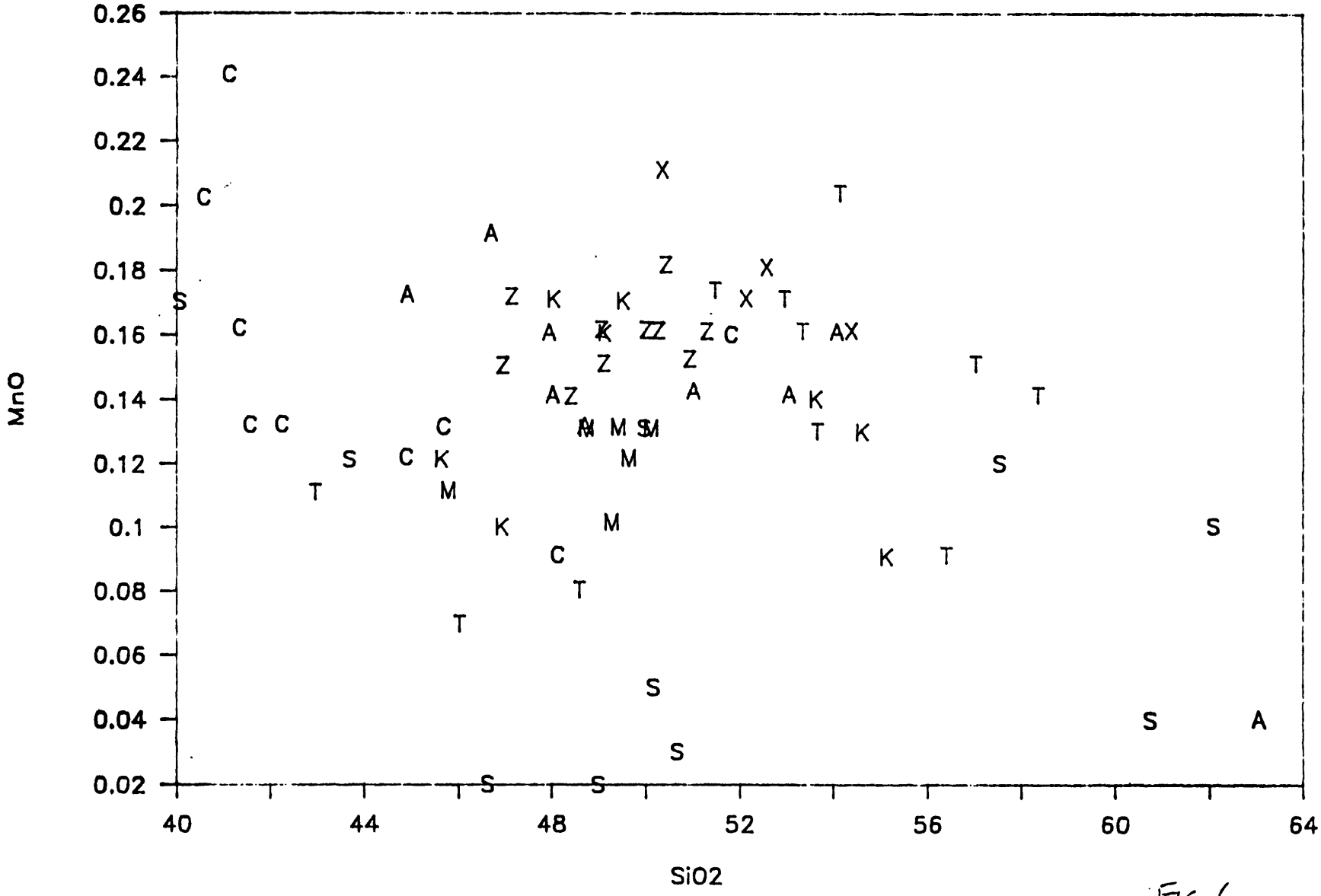
MnO
0.26
0.24
0.22
0.2
0.18
0.16
0.14
0.12
0.1
0.08
0.06
0.04
0.02
40
44
48
52
56
60
64
SiO2

Fig. 6

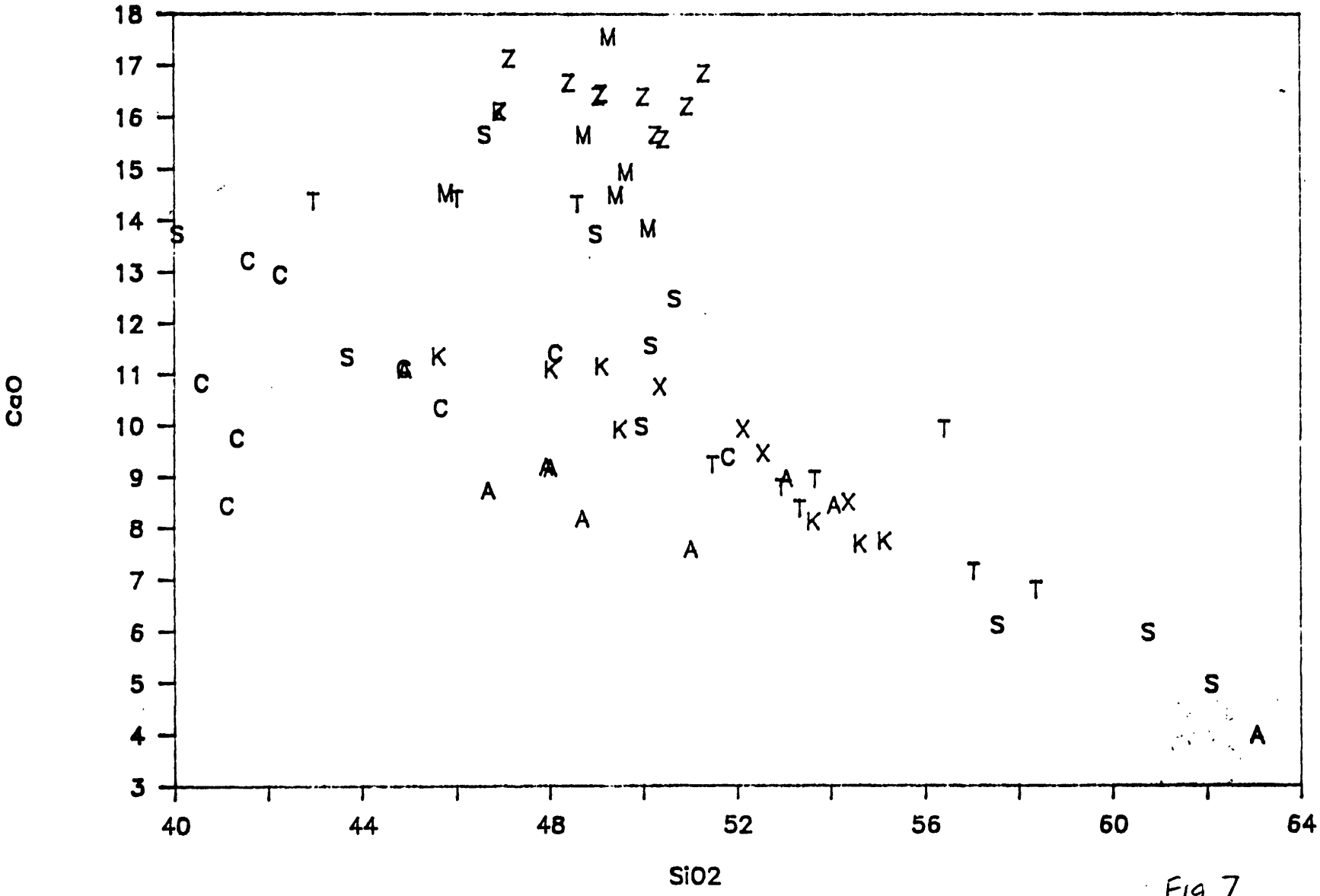

Fig 7

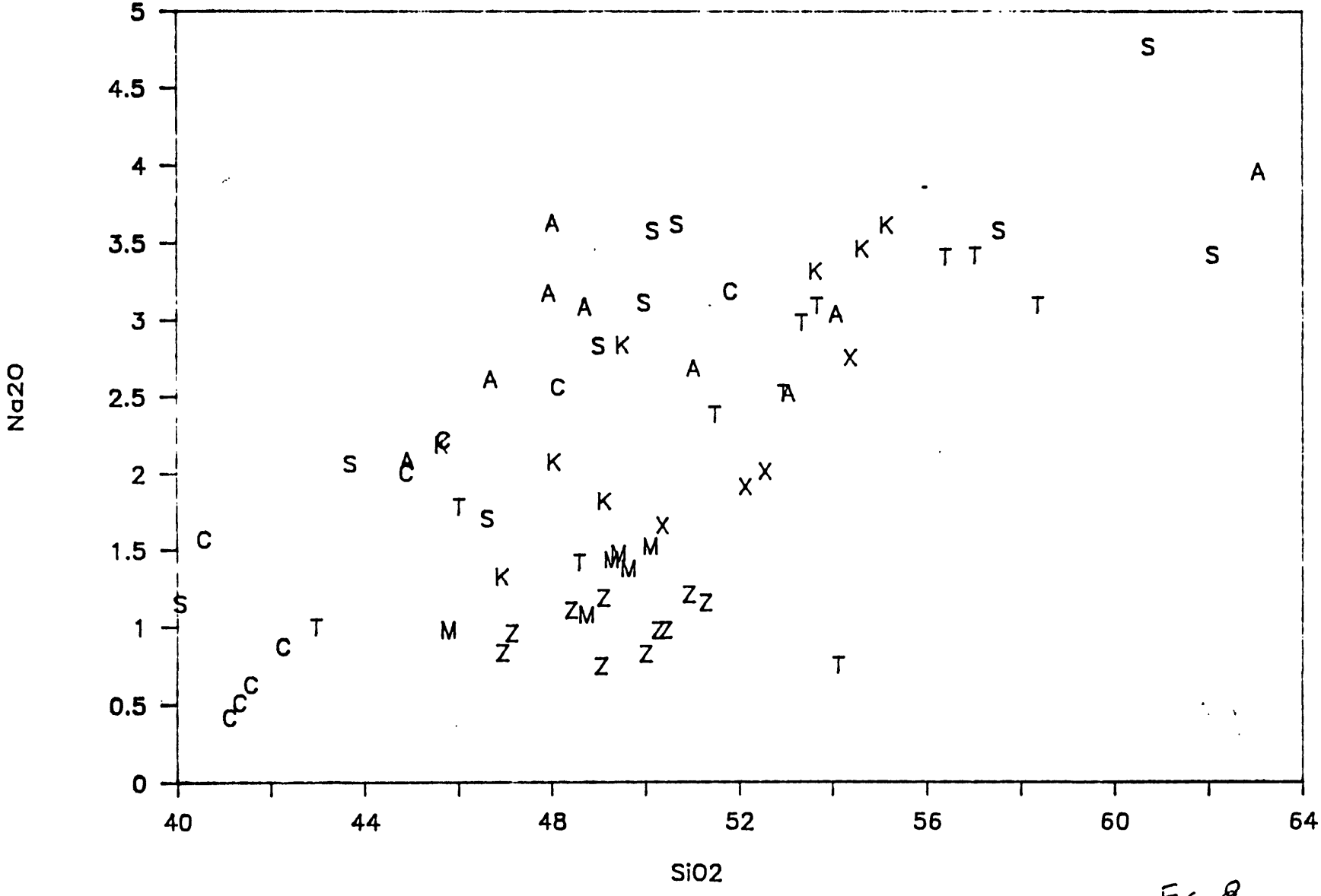

Fig. 8

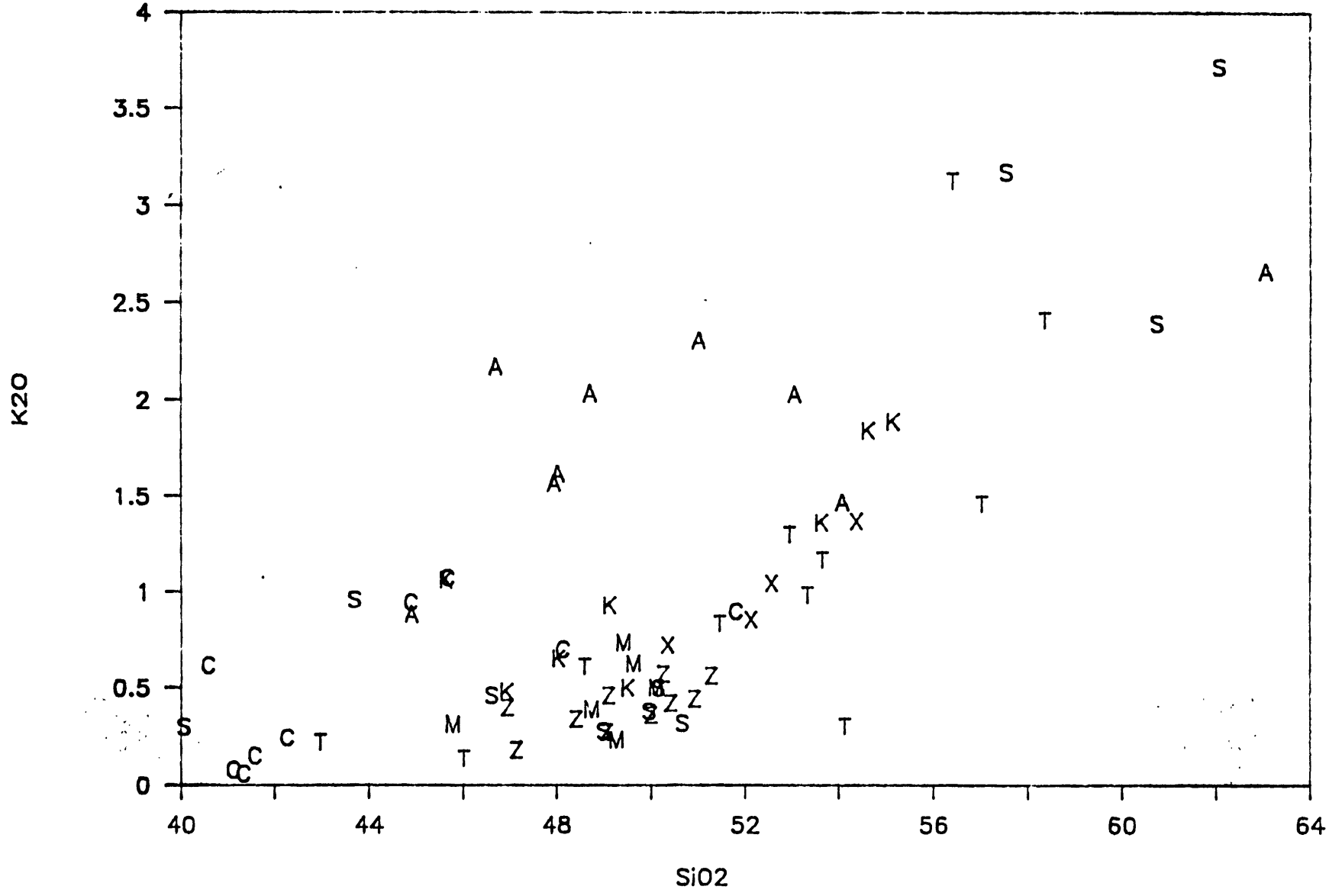

Fig. 9

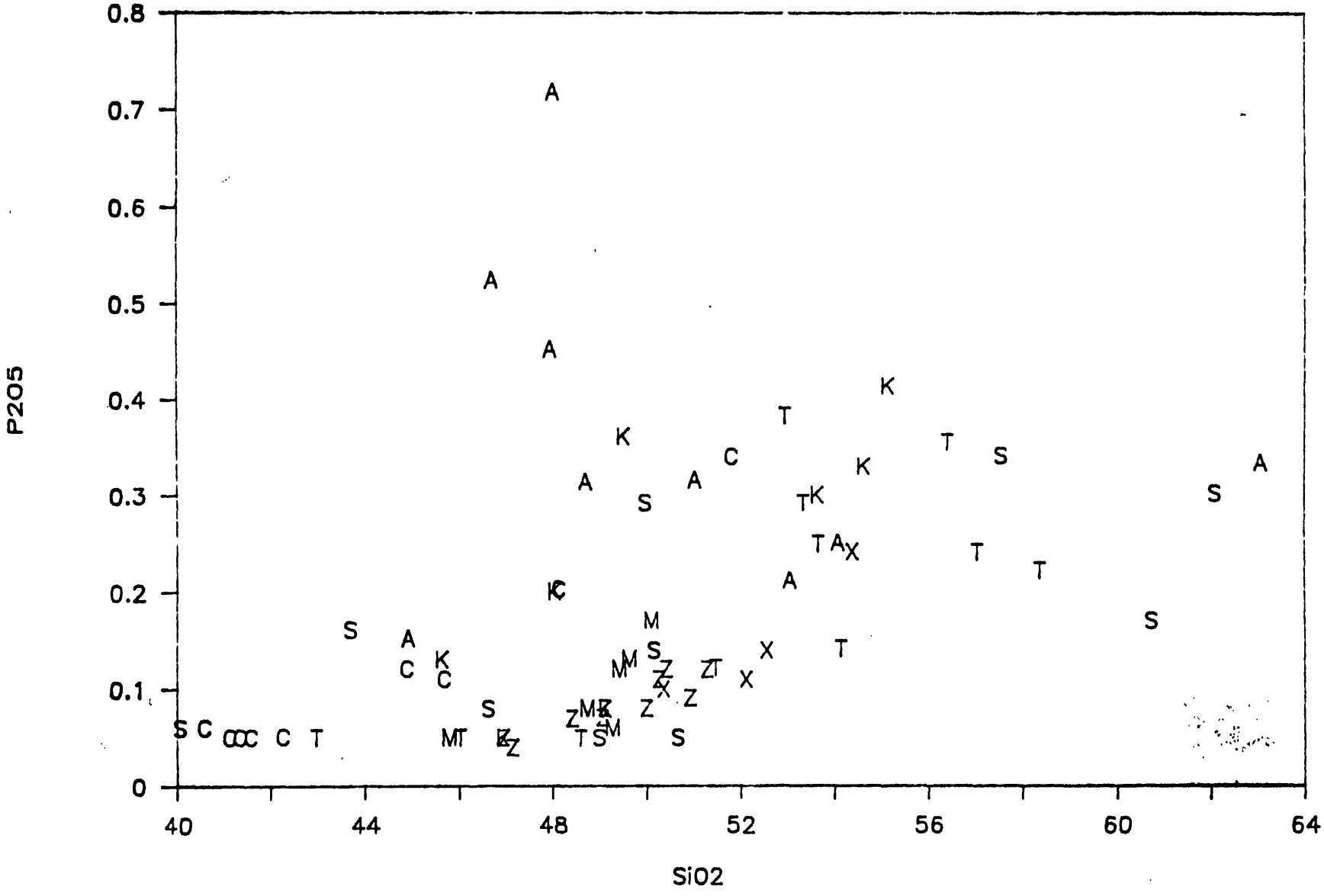

Fig 10

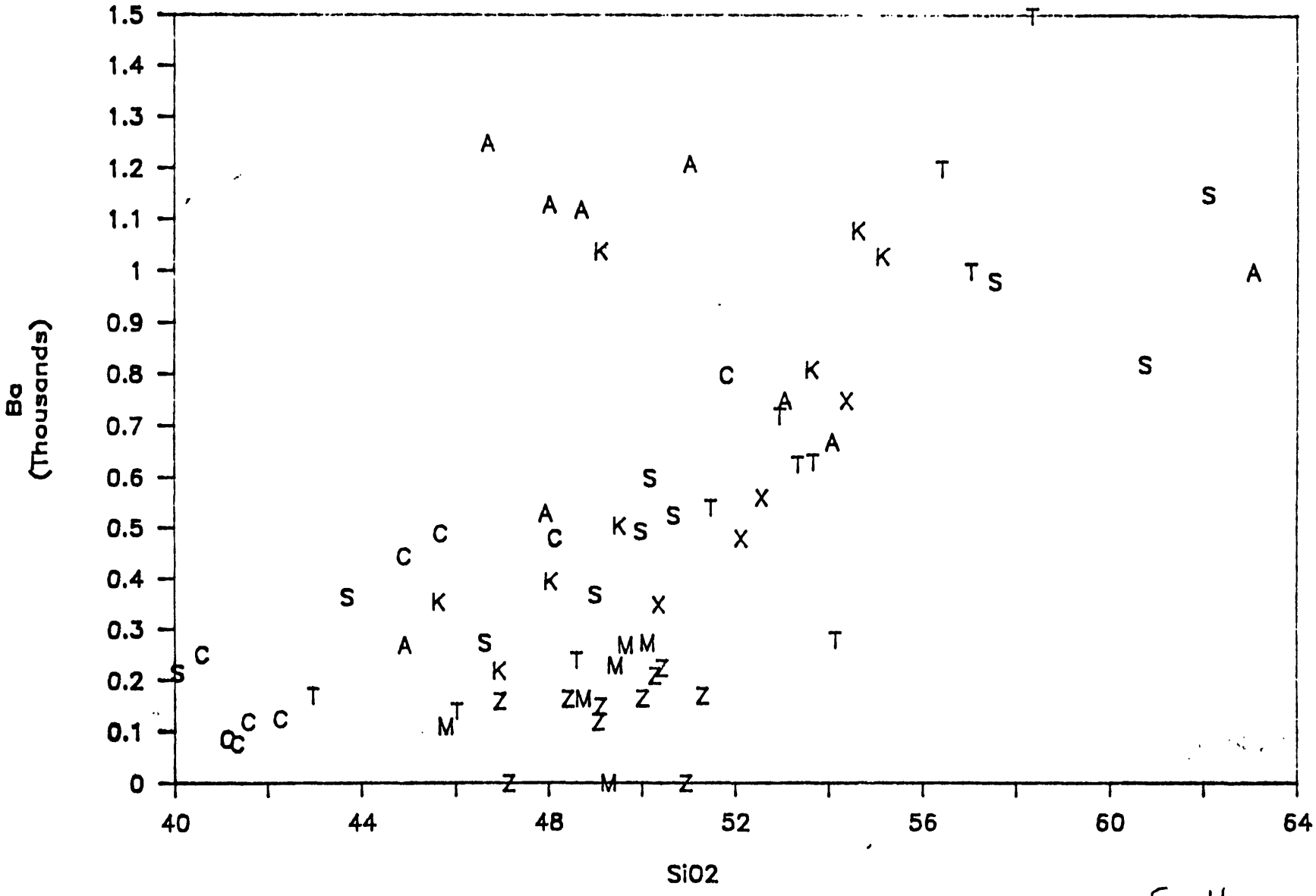
Ba
(Thousands)
1.5
1.4
1.3
1.2
1.1
1
0.9
0.8
0.7
0.6
0.5
0.4
0.3
0.2
0.1
0
40
44
48
52
56
60
64
SiO2

Fig 11

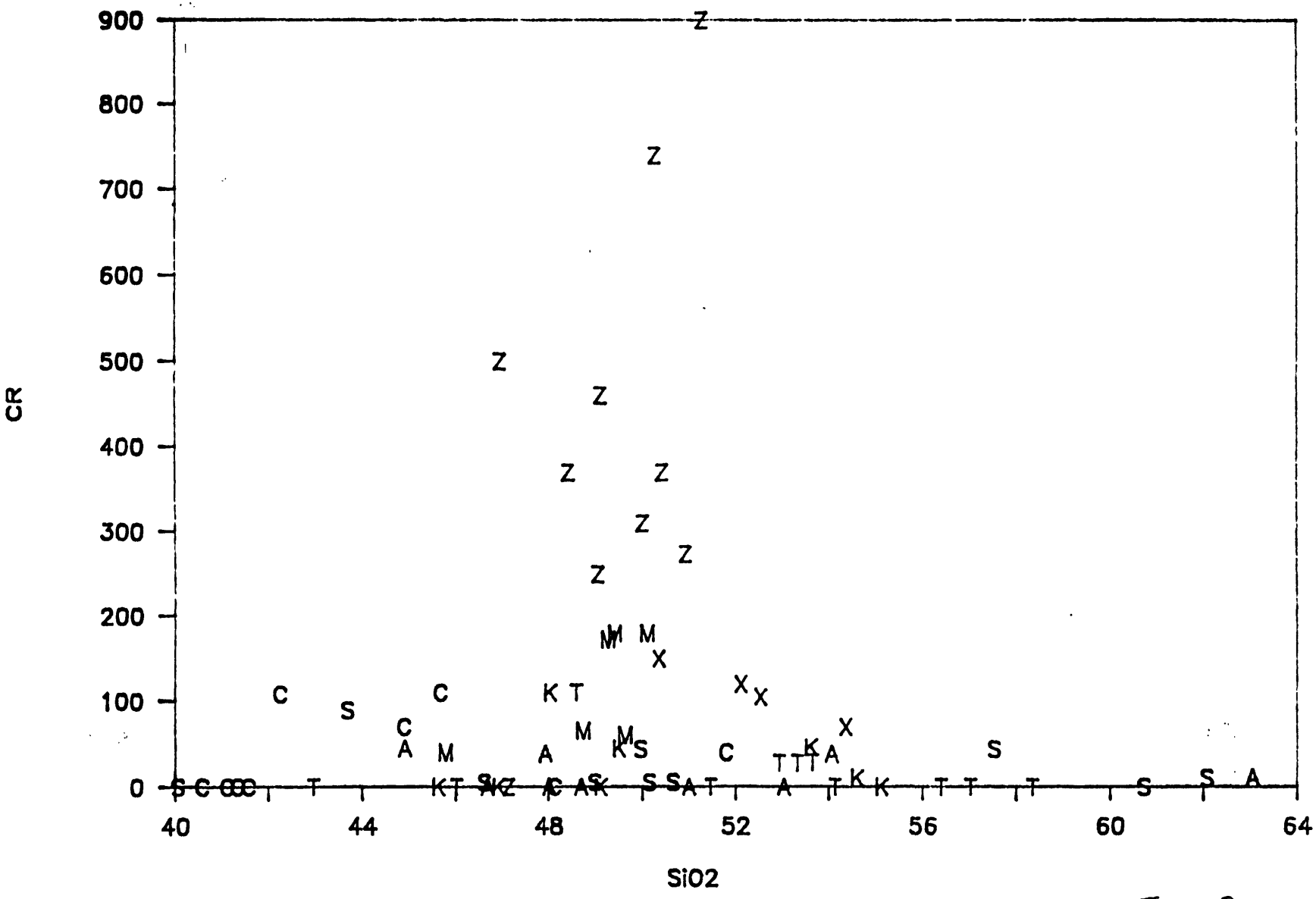

Fig 12

Cv = 0 → Cv not determined for those vox.

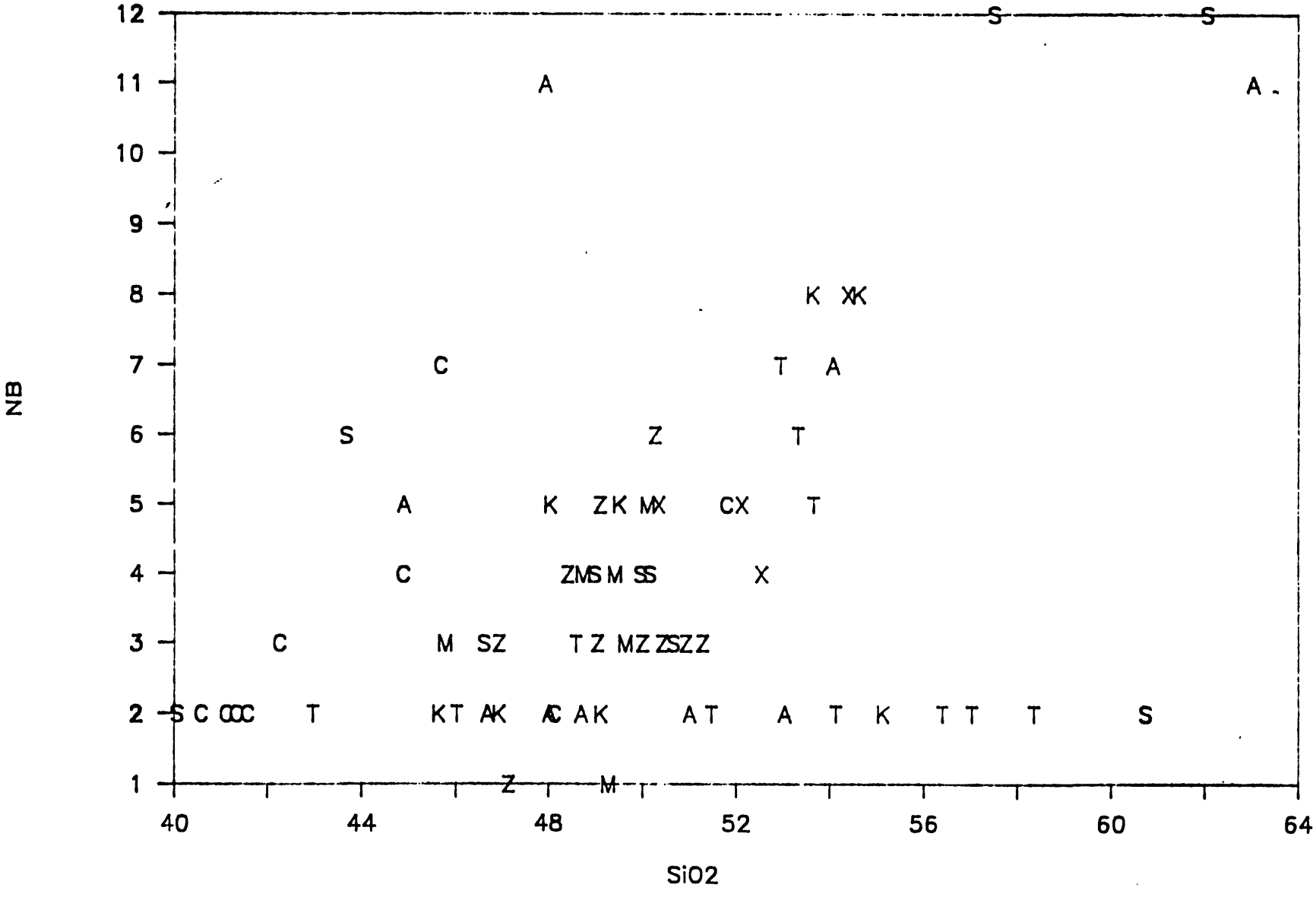

Fig 13

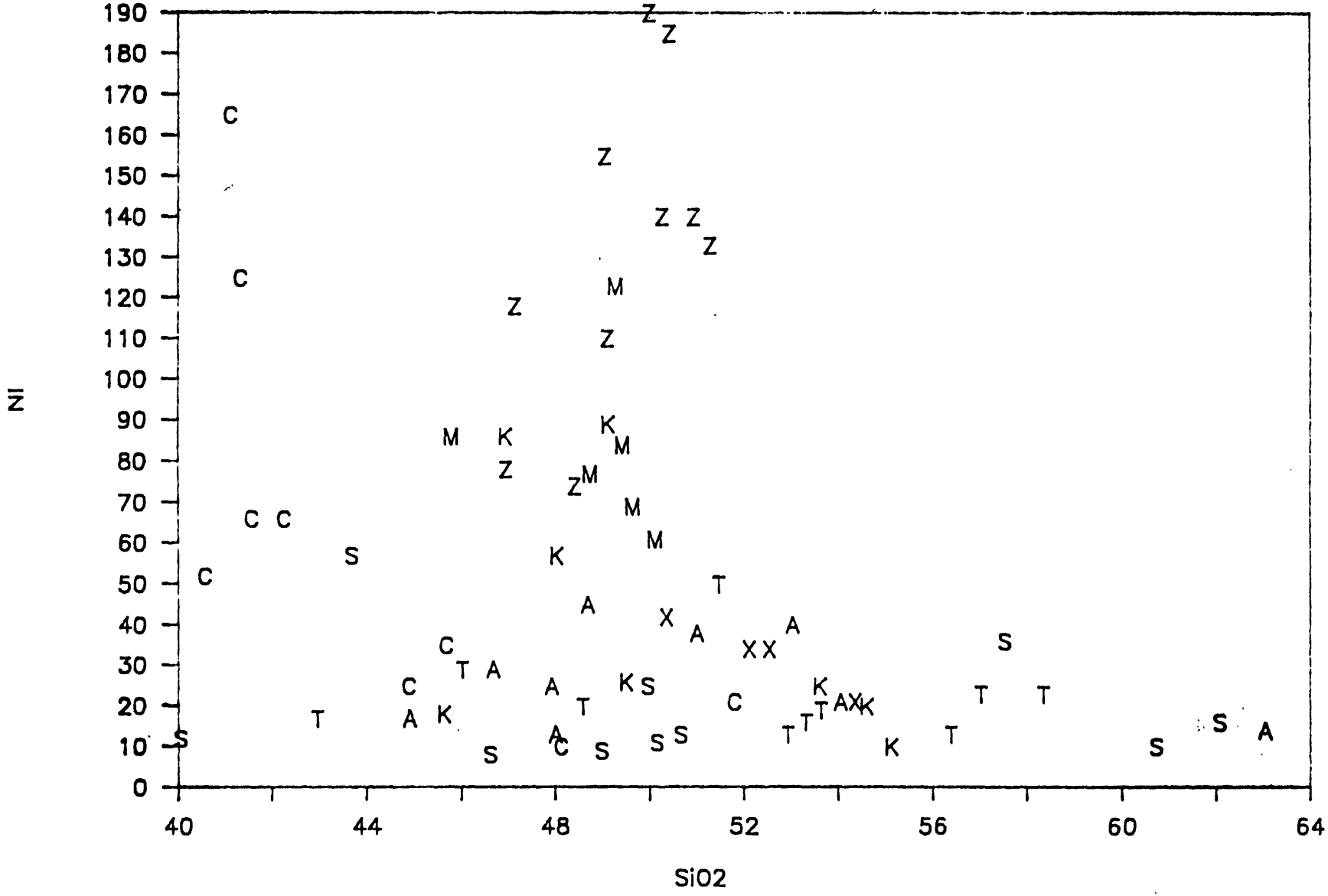
NI
SiO2
190
180
170
160
150
140
130
120
110
100
90
80
70
60
50
40
30
20
10
0
40
44
48
52
56
60
64

Fig 14

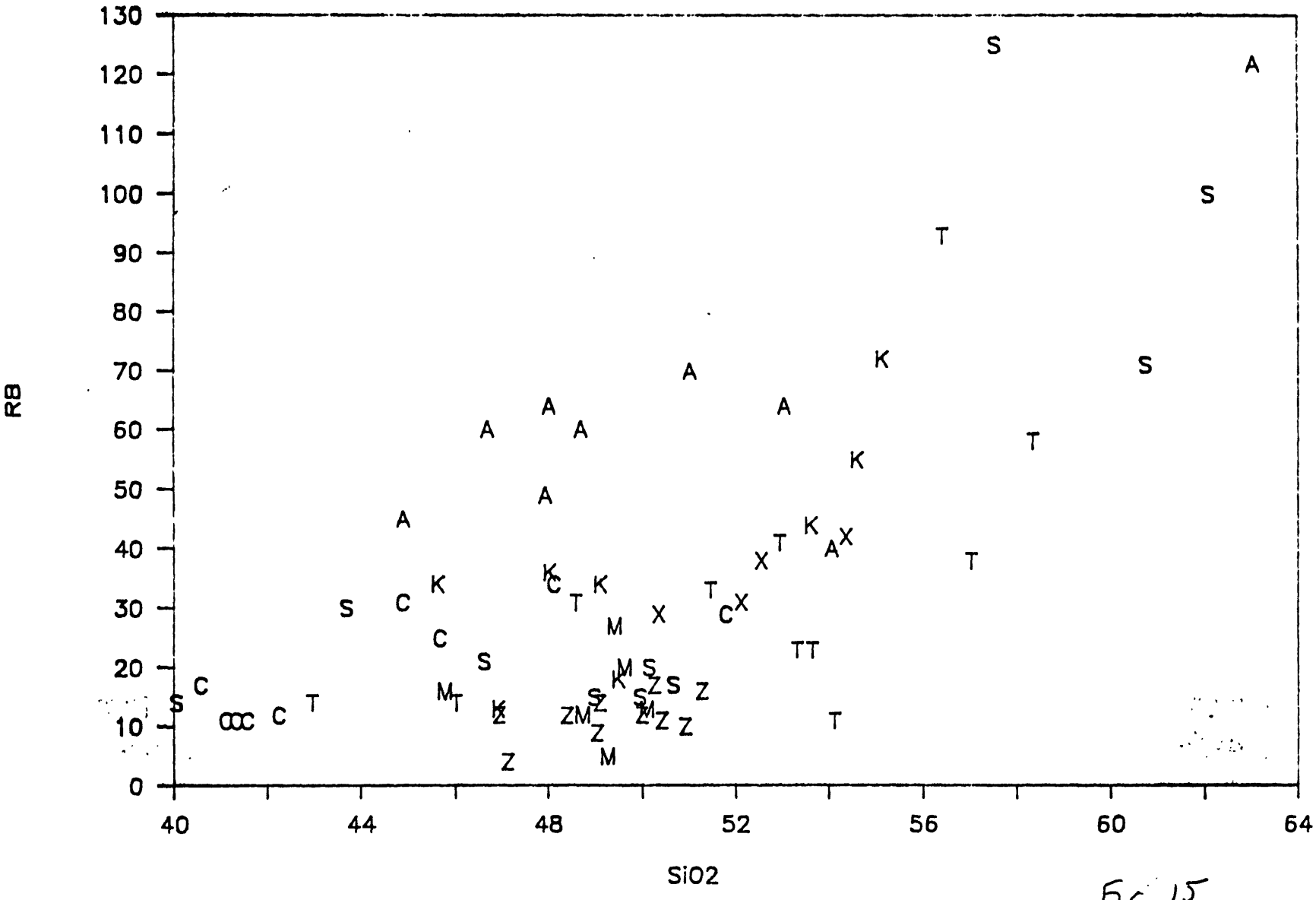
RB
SiO2
130
120
110
100
90
80
70
60
50
40
30
20
10
0
40
44
48
52
56
60
64

Fig. 15

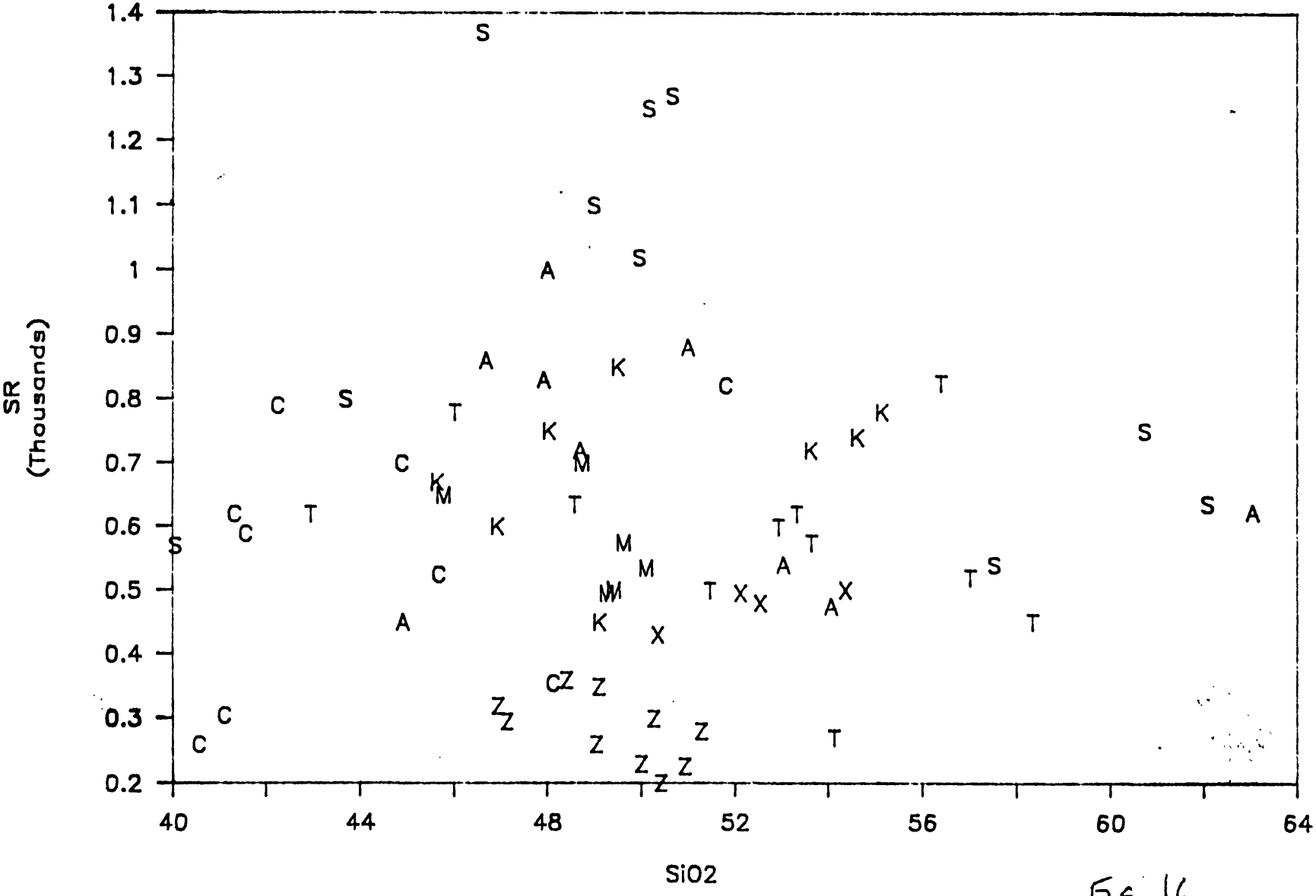
SR
(Thousands)
1.4
1.3
1.2
1.1
1
0.9
0.8
0.7
0.6
0.5
0.4
0.3
0.2
40
44
48
52
56
60
64
SiO2

Fig 16

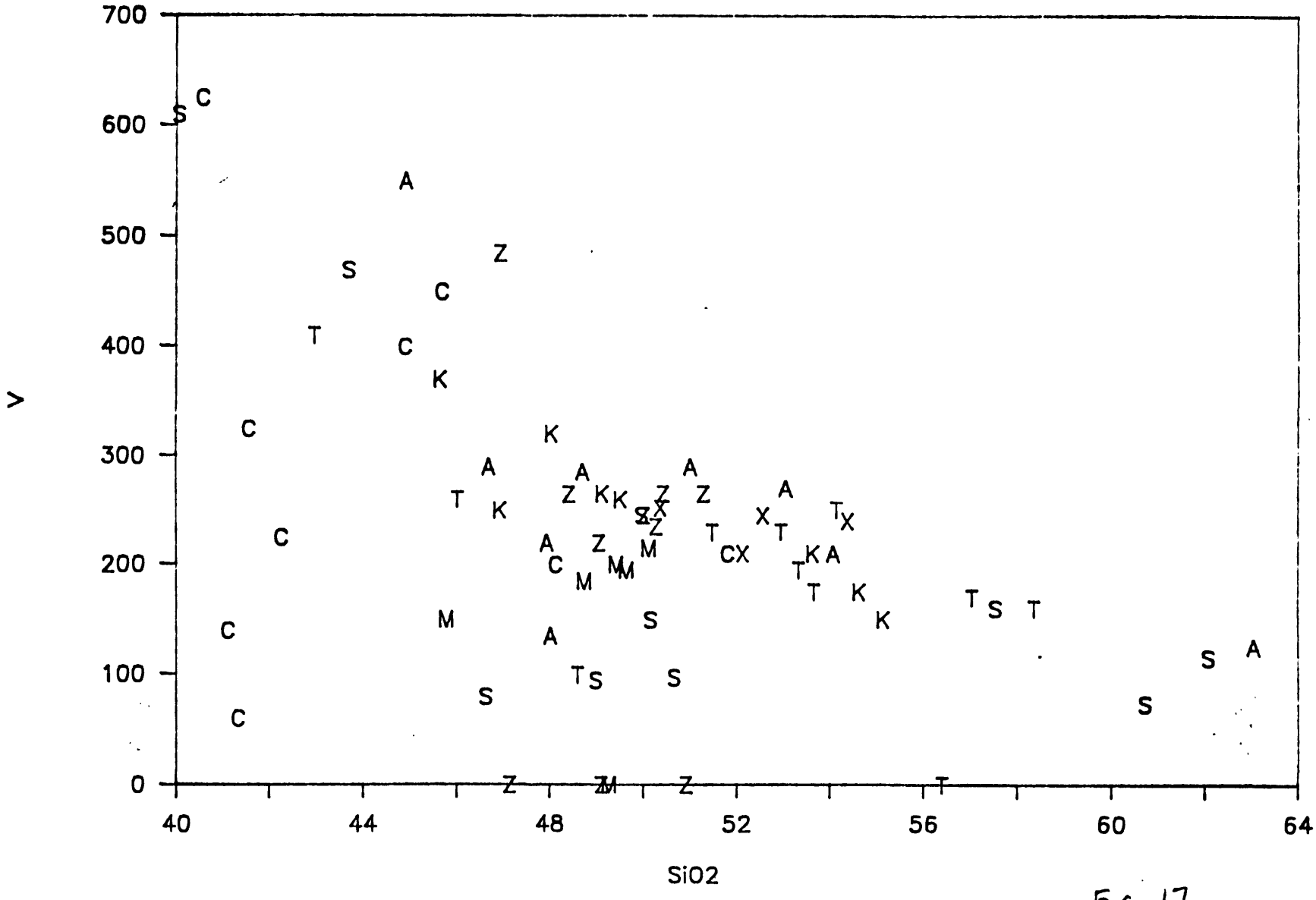

Fig 17

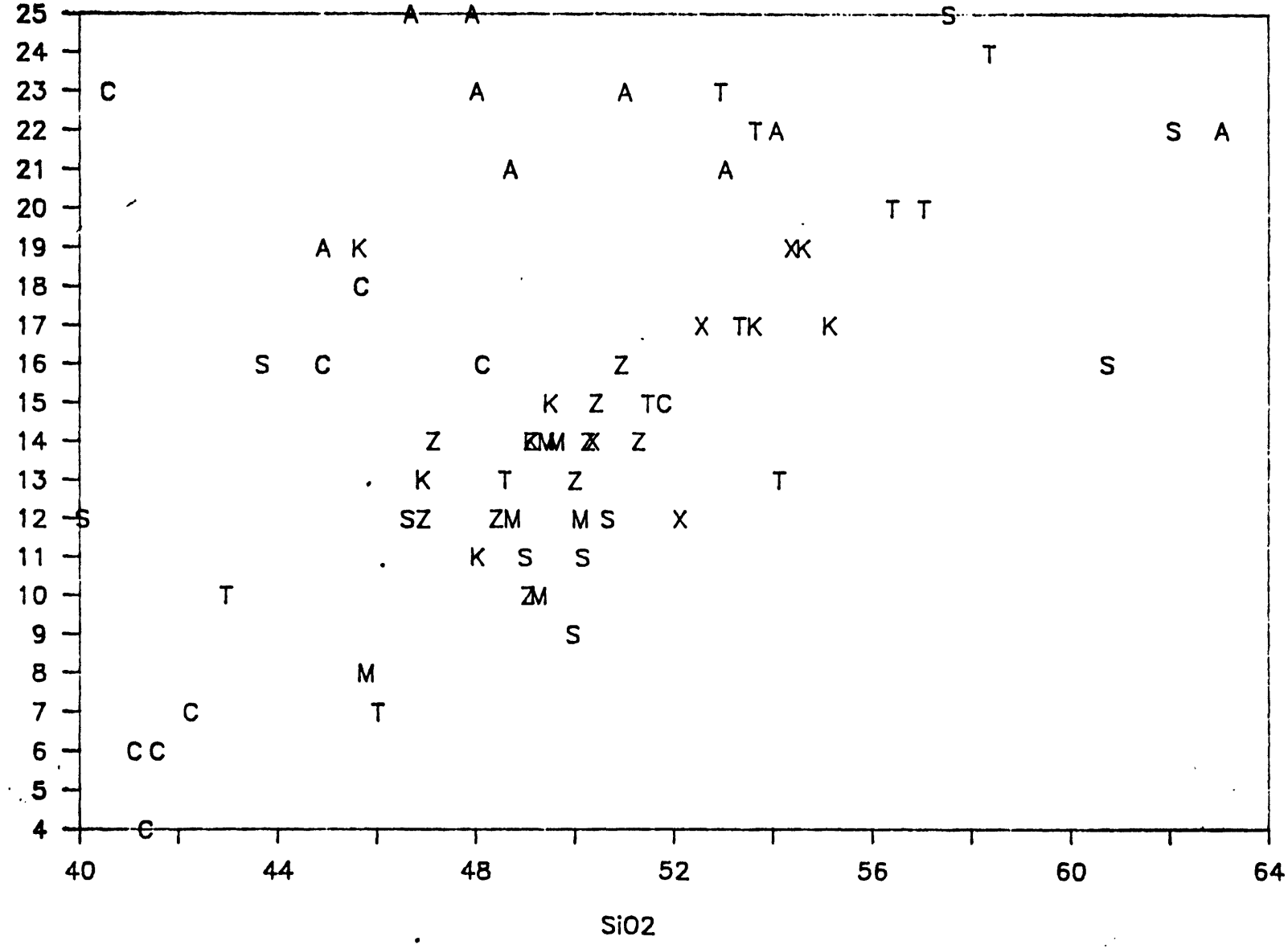
25
24
23
22
21
20
19
18
17
16
15
14
13
12
11
10
9
8
7
6
5
4
Y
40
44
48
52
56
60
64
SiO2

Fig 18

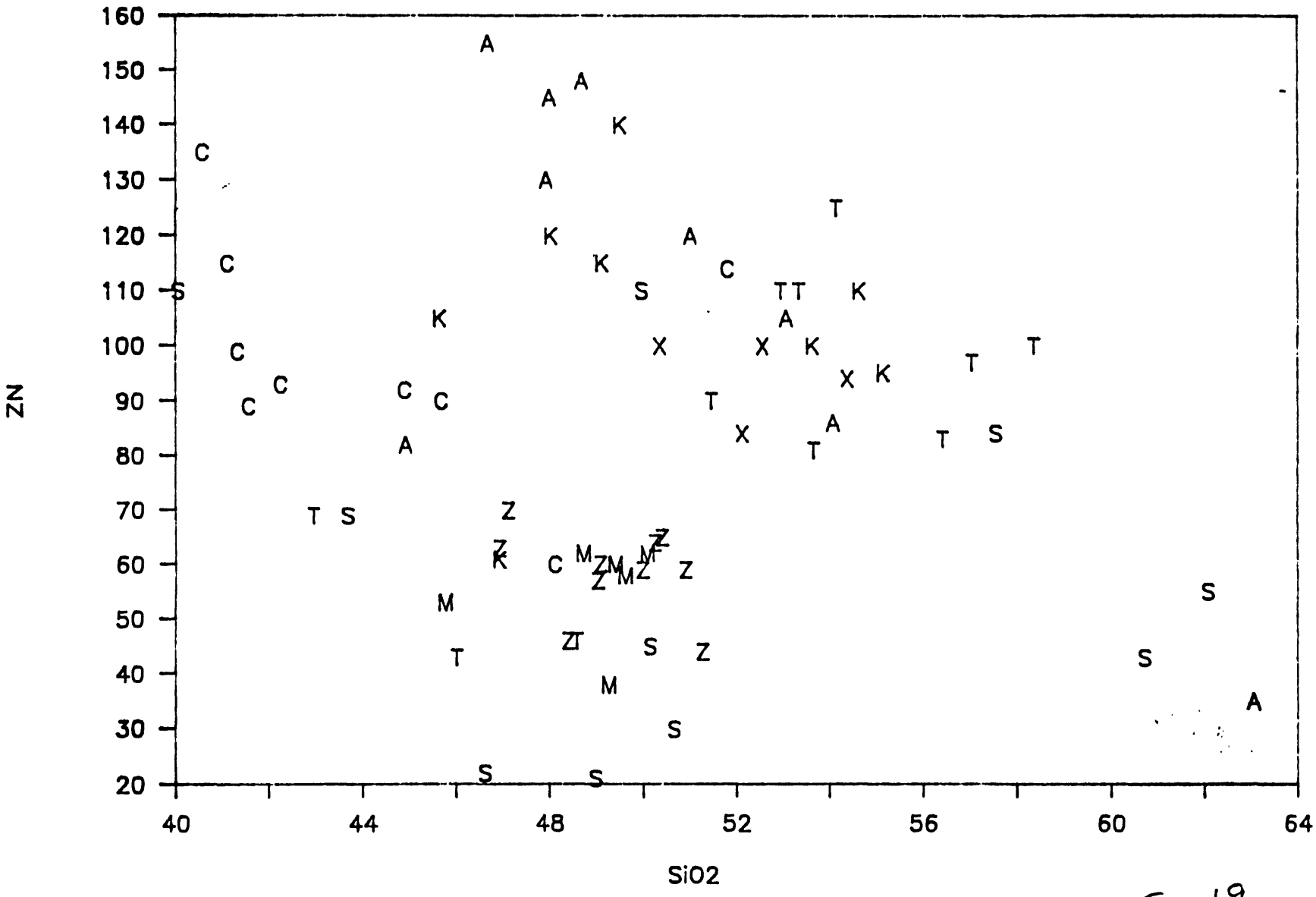
ZN
SiO2
160
150
140
130
120
110
100
90
80
70
60
50
40
30
20
40
44
48
52
56
60
64

Fig 19

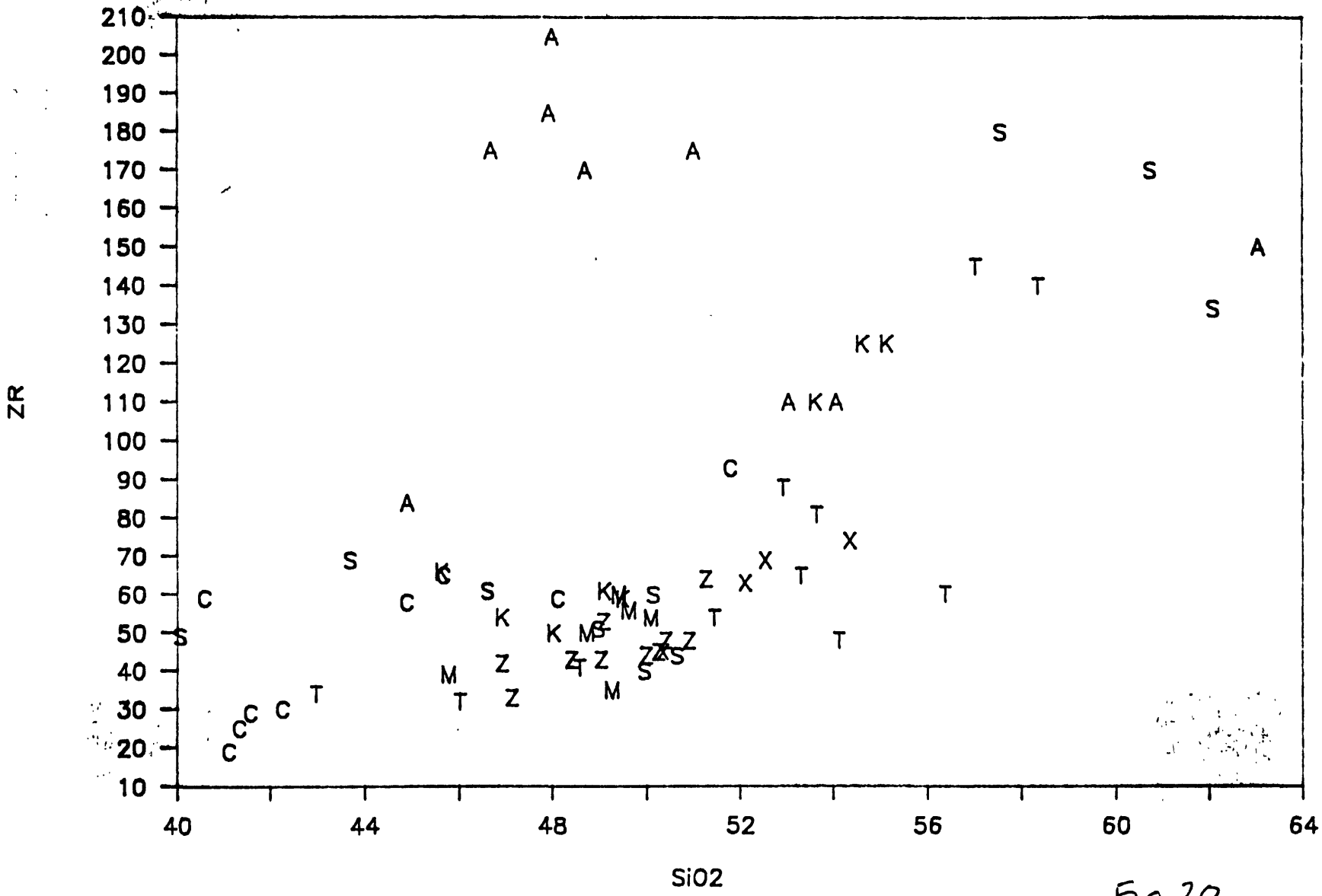
ZR
SiO2
210
200
190
180
170
160
150
140
130
120
110
100
90
80
70
60
50
40
30
20
10
40
44
48
52
56
60
64

Fig 20